INTEGRAL/IBIS 17-yr hard X-ray all-sky survey

Roman A. Krivonos,[1][*] Sergey Yu. Sazonov,[1,2] Ekaterina A. Kuznetsova,[1]
Alexander A. Lutovinov,[1] Ilya A. Mereminskiy,[1] and Sergey S. Tsygankov[1,3]

[1]*Space Research Institute (IKI), Profsoyuznaya 84/32, Moscow 117997, Russia*
[2]*Moscow Institute of Physics and Technology, Institutsky per. 9, 141700 Dolgoprudny, Russia*
[3]*Department of Physics and Astronomy, FI-20014 University of Turku, Finland*

ABSTRACT

The International Gamma-Ray Astrophysics Laboratory (*INTEGRAL*), launched in 2002, continues its successful work in observing the sky at energies $E > 20$ keV. The legacy of the mission already includes a large number of discovered or previously poorly studied hard X-ray sources. The growing *INTEGRAL* archive allows one to conduct an all-sky survey including a number of deep extragalactic fields and the deepest ever hard X-ray survey of the Galaxy. Taking advantage of the data gathered over 17 years with the IBIS coded-mask telescope of *INTEGRAL*, we conducted survey of hard X-ray sources, providing flux information from 17 to 290 keV. The catalog includes 929 objects, 890 of which exceed a detection threshold of 4.5σ and the rest are detected at $4.0 - 4.5\sigma$ and belong to known cataloged hard X-ray sources. Among the identified sources of known or suspected nature, 376 are associated with the Galaxy and Magellanic clouds, including 145 low-mass and 115 high-mass X-ray binaries, 79 cataclysmic variables, and 37 of other types; and 440 are extragalactic, including 429 active galactic nuclei (AGNs), 2 ultra-luminous sources, one supernova (AT2018cow) and 8 galaxy clusters. 113 sources remain unclassified. 46 objects are detected in the hard X-ray band for the first time. The Log$N$-Log$S$ distribution of 356 non-blazar AGNs is measured down to a flux of 2×10^{-12} erg s^{-1} cm^{-2} and can be described by a power law with a slope of 1.44 ± 0.09 and normalization 8×10^{-3} deg^{-2} at 10^{-11} erg s^{-1} cm^{-2}. The Log$N$-Log$S$ distribution of unclassified sources indicates that the majority of them are of extragalactic origin.

Key words: catalogs – surveys – X-rays: general.

1 INTRODUCTION

The *INTEGRAL* (Winkler et al. 2003) observatory has been successfully operating in orbit since its launch in 2002 October. The high sensitivity in the hard X-ray band ($\sim 20 - 100$ keV) and relatively good angular resolution of the IBIS coded-mask telescope (Ubertini et al. 2003) makes surveying the hard X-ray sky one of the primary goals of *INTEGRAL*. Over the past years, *INTEGRAL* has conducted many surveys, starting with sky areas of a few hundred squared degrees and gradually covering the entire celestial sphere (see Krivonos et al. 2021, for a review).

The *INTEGRAL* hard X-ray surveys have been used as a basis for studies of various classes of objects, from cataclysmic variables (CVs) and symbiotic stars (see Lutovinov et al. 2020, for a review), through low mass X-ray binaries (LMXB; see Sazonov et al. 2020, for a review) and high mass X-ray binaries (HMXB; see Kretschmar et al. 2019, for a review), to extragalactic objects, mainly active galactic nuclei (AGNs; see Malizia et al. 2020, for a review).

Since 2004, the sky has also been surveyed in hard X-rays by the Burst Alert Telescope (BAT; Barthelmy et al. 2005) of the *Neil Gehrels Swift Observatory* (*Swift*; Gehrels et al. 2004), which provides a nearly uniform all-sky coverage (see Oh et al. 2018, and references therein) with somewhat longer exposures at high Galactic latitudes. In contrast to *Swift*, the *INTEGRAL* observatory provides a sky survey with exposures that are deeper near the Galactic plane, which renders the *Swift*/BAT and *INTEGRAL*/IBIS hard X-ray surveys complementary to each other.

Krivonos et al. (2007b) presented the first *INTEGRAL*/IBIS all-sky survey based on 3.5 years of observations at the beginning of the mission. The catalog of sources detected in the 17–60 keV energy band comprises 403 objects, 316 of which were found above a threshold of 5σ on the time-averaged sky map, and the rest were detected in various subsamples of observations. The most recent data release of the *INTEGRAL*/IBIS catalog with all-sky coverage, presented by Bird et al. (2016), was based on the first 1000 orbits of *INTEGRAL*, i.e. the data acquired from the launch at the end of 2002 until the end of 2010. This catalog includes 939 sources detected above a significance threshold of 4.5σ in the $17 - 100$ keV energy band on sky maps with different exposures.

In this work, we extend the *INTEGRAL*/IBIS all-sky survey to 17 years, using the whole set of observations carried out between 2002 December and 2020 January. We obtain a statistically clean catalog of hard X-ray sources detected above the 4.5σ threshold along with their classification, if available. This list includes 46 newly detected sources. We also provide a sample of sub-threshold, $4.0 - 4.5\sigma$, *INTEGRAL* sources that were already known from previous *INTEGRAL* and *Swift* hard X-ray catalogs. In total, the final catalog comprises 929 hard X-ray sources.

[*] E-mail: krivonos@cosmos.ru (IKI)

2 DATA ANALYSIS

For the current hard X-ray survey, we utilized all publicly available *INTEGRAL* data acquired by the ISGRI low-energy detector layer (Lebrun et al. 2003) of the IBIS telescope between 2002 December and 2020 January (spacecraft revolutions 26–2180). This corresponds to a total nominal exposure time of 406 Ms. We reduced the IBIS/ISGRI data with the *INTEGRAL* data analysis software developed at IKI[1] (see e.g., Krivonos et al. 2010a, 2012; Churazov et al. 2014, and references therein). Below we describe details of the data analysis that are relevant for the current work.

We first applied the latest energy calibration (Caballero et al. 2013) for the registered IBIS/ISGRI detector events with the INTEGRAL Offline Scientific Analysis (OSA) provided by the INTEGRAL Science Data Centre (ISDC) Data Centre for Astrophysics up to the COR level. Because the latest OSA version 11.0 is only applicable to the data obtained since 26 December 2015 (revolution 1626), we calibrated ISGRI events obtained within the orbit ranges of 26–1625 and 1626–2180 with OSA versions 10.2 and 11.0, respectively,

We then produced a sky image of every individual *INTEGRAL* observation with a typical exposure time of 2 ks (referred as a *Science Window*, or *ScW*). The flux scale in each *ScW* sky image was adjusted to the flux of the Crab nebula measured in the nearest observation. This procedure was applied to account for the loss of sensitivity at low energies $E \lesssim 25$ keV caused by ongoing detector degradation.

2.1 Energy bands

To be consistent with our previous works, we chose 17–60 keV as a working energy band for detection of sources in the present hard X-ray survey. This also allows us to utilize the time period of spacecraft orbits before ~ 1000 when ISGRI had good sensitivity in the $\sim 17 - 30$ keV band. To determine an energy range that is not affected by detector aging, we analyzed the long-term (2003-2019) light curve of the persistent X-ray source Ophiuchus cluster in different energy bands and found that at energies above 30 keV ISGRI demonstrates stable efficiency over the whole period of observations (Kuznetsova et al. 2022). We selected 30–80 keV as an additional energy range for studying source light curves. Finally, in order to provide rough broad-band spectral information, we analysed the sky in logarithmically spaced energy bands of 17–26, 26–38, 38–57, 57–86, 86–129, 129–194 and 194–290 keV. Table 1 contains the list of the used energy bands and conversion factors between physical and mCrab units assuming the Crab spectrum in the form of $10(E/1\,\mathrm{keV})^{-2.1}$ photons cm^{-2} s^{-1} keV^{-1}.

2.2 Sky map mosaics

After applying selection criteria over the list of reconstructed *ScW* sky images, as described in Krivonos et al. (2007b), we obtained 157, 200 *ScWs* in each energy band, which comprises 273 Ms of dead-time corrected exposure. Finally, we projected the sky images of all *ScWs* on to 25° × 25° sky frames covering the whole sky in the HEALPIX reference grid (Górski et al. 2005), with 192 frames in total.

The procedure of sky reconstruction for IBIS/ISGRI suffers from systematic noise, which is mainly caused by the presence of bright sources in the field of view (FOV) (see e.g., Krivonos et al. 2007c,

Table 1. Working energy bands for the current *INTEGRAL* all-sky survey.

Name	Range [keV]	Width [keV]	1 mCrab [erg s^{-1} cm^{-2}]	[ph cm^{-2} s^{-1}]
E1	17 – 60	43	1.43×10^{-11}	3.02×10^{-4}
E2	30 – 80	50	1.06×10^{-11}	1.42×10^{-4}
E3	17 – 26	9	5.02×10^{-12}	1.50×10^{-4}
E4	26 – 38	12	4.31×10^{-12}	8.61×10^{-5}
E5	38 – 57	19	4.42×10^{-12}	5.98×10^{-5}
E6	57 – 86	29	4.31×10^{-12}	3.87×10^{-5}
E7	86 – 129	43	4.08×10^{-12}	2.43×10^{-5}
E8	129 – 194	65	3.94×10^{-12}	1.57×10^{-5}
E9	194 – 290	96	3.73×10^{-12}	9.89×10^{-6}

2012). As a result, some sky artefacts are still present around persistent bright sources, such as Crab, Sco X–1, Cyg X–1, Cyg X–3, Vela X–1, GX 301–2 and GRS 1915+105, which requires manual inspection of the list of source candidates. Apart from the bright persistent sources, sky regions can be seriously contaminated by bright Galactic transients, which, however, can be excluded from the analysis. To produce sky maps that are as clean as possible, we avoided observations with angular offsets closer than 20° from the following bright transients: IGR J17480–2446 (1519 – 1530, Bordas et al. 2010), GRS 1716–249 (1780 – 1806, Bassi et al. 2019), MAXI J1535–571 (1860 – 1865, Russell et al. 2019; Parikh et al. 2019), Swift J174510.8–262411 (1212 – 1264, Del Santo et al. 2016), MAXI J1820+070 (1931 – 1952, Shidatsu et al. 2018) and MAXI J1348–630 (2050 – 2061, Yatabe et al. 2019), where the range in parenthesis means the interval of excluded spacecraft orbits.

2.3 Detection of sources

Sources were searched as excesses on 25° × 25° ISGRI sky frames, convolved with a Gaussian with $\sigma = 5'$, which approximates the effective point spread function (PSF) of IBIS/ISGRI. The signal-to-noise (S/N) distribution of pixels is dominated by the statistical noise and can be described by a Gaussian with zero mean and unit variance, as demonstrated in our previous works (e.g., Krivonos et al. 2007b). However, in sky regions that contain very bright point sources or the crowded field near the Galactic center, the root-mean-square (RMS) scatter of the S/N distribution increases (e.g., Krivonos et al. 2010a), which requires manual inspection of detected excesses, as was already noted above.

We considered two criteria for detecting sources. First, a source is considered to be detected if the significance of its detection exceeds 4.5σ. Given the IBIS/ISGRI angular resolution of $12'$, the all-sky map may be regarded as consisting of $\sim 10^6$ statistically independent pixels, which implies that less than 10 false detections are expected to be registered due to statistical fluctuations. The second, alternative, criterion, is intended to increase the completeness of the survey with respect to previously known hard X-ray sources that fall slightly below the 4.5σ detection threshold. Specifically, if the spatial position of an *INTEGRAL* source candidate detected with a significance of $4.0 - 4.5\sigma$ is consistent with that of a known hard X-ray source from an external catalog it is considered to be detected. To this end, we cross-correlated the list of $S/N > 4.0\sigma$ source candidates with previous *INTEGRAL*/IBIS and *Swift*/BAT hard X-ray source catalogs that are listed in Table 2. The search was done within a radius of
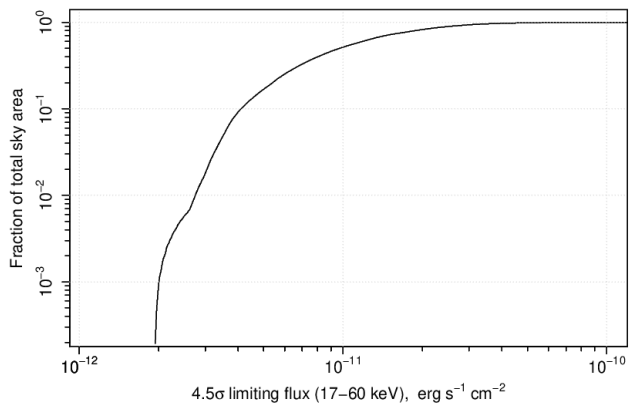
Figure 1. Fraction of the total sky area surveyed as a function of the limiting flux for source detection with 4.5σ significance in the 17–60 keV energy band.

$10'$. Table 2 also provides the number of cross-matches with a given catalog.

As a result, all $4.0 < S/N < 4.5$ sources included in the final catalog are known hard X-ray sources. Consequently, we mark $S/N > 4.5\sigma$ sources that do not have a counterpart in any of the hard X-ray surveys listed in Table 2 as newly detected in hard X-rays, except for a number of known X-ray transients and historical X-ray sources that are not listed in the mentioned hard X-ray catalogs for some reason. There are in total 46 newly detected hard X-ray sources.

2.4 Survey sensitivity

Figure 1 shows the survey sky coverage as a function of the flux corresponding to the 4.5σ significance limit. The peak sensitivity, reached in the Galactic Center region, is about 0.14 mCrab (2×10^{-12} erg s^{-1} cm^{-2}) in the $17 - 60$ keV energy band. Compared to our previous work based on 14 years of data (Krivonos et al. 2017) the peak sensitivity in this band has improved by nearly 10%. The present survey covers 10% of the sky down to a flux limit of ~ 0.3 mCrab (4.3×10^{-12} erg s^{-1} cm^{-2}) and 90% of the sky down to ~ 1.8 mCrab (2.6×10^{-11} erg s^{-1} cm^{-2}) in the $17 - 60$ keV energy band. A limiting (4.5σ) flux of 1 mCrab or better is achieved for $\sim 70\%$ of the sky.

3 CATALOG OF SOURCES

The catalog of detected sources was compiled in the reference $17 - 60$ keV energy band following the detection criteria described in Section 2.3. In addition, Table 3 provides source counts statistics for all energy bands considered in this work. The list of sources detected in the $17 - 60$ keV band is presented in Table A1 in Appendix A, and its content is described below.

Column (1) "Id" – sequence number of the source in the current catalog.

Column (2) "Name" – name of the source. Common names are given for sources which were known before their detection with *INTEGRAL*. Sources discovered by *INTEGRAL* or those whose nature was established thanks to the *INTEGRAL* observations are named as "IGR".

Columns (3,4) "RA, Dec" – source equatorial (J2000) coordinates. The positional accuracy depends on the significance of detection

by IBIS/ISGRI (Gros et al. 2003; Bird et al. 2007). According to Krivonos et al. (2007b), the estimated 68% confidence intervals for sources detected at $5 - 6$, 10, and $> 20\sigma$ are $2.1'$, $1.5'$, and $< 0.8'$, respectively.

Column (5) "Flux" – time-averaged flux of the source in the $17 - 60$ keV energy band. The online version of the table also contains source fluxes in all energy bands listed in Table 1.

Column (6) "Type" – general astrophysical type of the object. LMXB (HMXB) – low- (high-) mass X-ray binary; X-RAY BINARY – X-ray binary of uncertain type; CV – cataclysmic variable or symbiotic binary; SNR – supernova remnant; SNR/Pulsar – supernova remnant with a central pulsar (when both may contribute to the hard X-ray emission); MAGNETAR – magnetar (anomalous X-ray pulsars and soft gamma-ray repeaters); SUPERNOVA – supernova; STAR – active star (of various types, excluding the previously listed types of stellar objects); ULX – ultraluminous X-ray source; SEYFERT – AGN of the Seyfert or LINER type; BLAZAR – beamed AGN (BL Lac objects and flat-spectrum radio quasars); AGN – unclassified AGN (i.e., the object is known to be an AGN in a general sense but detailed optical classification is missing); CLUSTER – a cluster of galaxies; and UNIDENT – an unclassified object. A question mark indicates that the specified type is not firmly established. These classifications are mainly based on the information contained in the Simbad[2] and NED[3] databases as well as in the previous versions of the *INTEGRAL*/IBIS and *Swift*/BAT hard X-ray source catalogs (see Table 2). In addition, we strove to select the most recent and reliable source identifications from the literature if necessary.

Column (7) "Notes" – additional notes such as references, redshift information, alternative source names, spatial confusion and transient flags. The references are mainly provided for recently discovered sources and are related to determination of their nature. The redshifts of the extragalactic sources were adopted from SIMBAD, NED and the *Swift*/BAT AGN Spectroscopic Survey (BASS) (see Ricci et al. 2017, and references therein).

4 DISCUSSION AND SUMMARY

In this work we present the all-sky survey of hard X-ray sources in the reference $17 - 60$ keV energy band, based on the data archive of the IBIS coded-mask telescope on board the *INTEGRAL* observatory accumulated over 17 years, from 2002 December to 2020 January. The combined catalog of sources includes 929 objects, 890 of which exceed a detection threshold of 4.5σ and the rest are known hard X-ray sources detected at $4.0\sigma < S/N < 4.5\sigma$.

4.1 Properties of the catalog

Table 4 presents source statistics by astrophysical type and Table 5 lists source counts over three categories: Galactic objects, sources located in the Large and Small Magellanic Clouds, and extragalactic objects. 113 sources from the catalog remain unclassified.

We mark 46 sources detected at $S/N > 4.5\sigma$ as newly detected in hard X-rays since they do not have a counterpart in any of the selected hard X-ray catalogs (Table 2). We cross-correlated these sources with a number of catalogs in the soft X-ray band, namely the *ROSAT*

---

[2] Simbad Astronomical Database http://simbad.u-strasbg.fr
[3] NASA/IPAC Extragalactic Database http://ned.ipac.caltech.edu

Table 2. List of selected hard X-ray catalogs used for cross-matching.

X-ray survey	Band (keV)	Sources	Cross-matches[a]	Reference
Swift/BAT				
all-sky, 70 months	14–195	1210	617 (+20)	Baumgartner et al. (2013)
all-sky, 105 months	14–195	1632	693 (+18)	Oh et al. (2018)
INTEGRAL/IBIS				
1st catalog	20–100	123	122 (+6)	Bird et al. (2004)
~50% of sky, 2nd cat.	20–100	209	197 (+8)	Bird et al. (2006)
~70% of sky, 3rd cat.	17–100	421	358 (+12)	Bird et al. (2007)
all-sky, 4th catalog	17–100	723	485 (+12)	Bird et al. (2010)
all-sky, 1000 orbits	17–100	939	629 (+14)	Bird et al. (2016)
all-sky 3.5 years	17–60	403	369 (+13)	Krivonos et al. (2007b)
all-sky, 7 years	17–60	521	486 (+15)	Krivonos et al. (2010b)
$|b| < 17.5°$, 9 years	17–80	402	387 (+13)	Krivonos et al. (2012)
$|b| < 17.5°$, 14 years	17–60	72	70 (+2)	Krivonos et al. (2017)
deep extragal. fields	17–60	147	140 (+4)	Mereminskiy et al. (2016)

[a] The result of cross-correlation is regarded as positive if at least one source from the *INTEGRAL*/IBIS 17-year catalog is found within $10'$ from a source in the external catalog. The number of cases where there is more than one *INTEGRAL* source within $10'$ from the same source in the external catalog is given in brackets.

Table 3. Source detection statistics in different energy bands (see Table 1 for reference) of the current *INTEGRAL*/IBIS 17-year all-sky survey.

Band	S/N > 4.5	4.0 > S/N > 4.5[a]	Total
E1	890	39	929
E2	693	40	733
E3	554	45	599
E4	700	55	755
E5	597	48	645
E6	314	33	347
E7	208	29	237
E8	63	9	72
E9	17	5	22

[a] Such sources are required to have been previously detected in any of the all-sky hard X-ray surveys listed in Table 2.

Table 4. Statistics of sources in the catalog.

Type	Count (Notes)
LMXB	145
HMXB	115
X-ray binary (unclassified)	1 (SWIFT J1858.6-0814)
CV	79
Star	4
Magnetar	5
SNR, SNR/Pulsar	25
Molecular cloud	1 (Sgr B2)
Galactic Center	1 (Sgr A*)
Supernova	1 (AT2018cow)
ULX	2
Seyfert galaxy	336
AGN (unclassified)	39
Blazar	54
Galaxy cluster	8
Unidentified	113

Table 5. Statistics of identified sources by category.

Category	Count
Galactic	356
Magellanic Clouds	20
Extragalactic	440

all-sky bright source catalog (1RXS; Voges et al. 1999), the *XMM–Newton* slew survey (XMMSL2; Saxton et al. 2008), the *XMM–Newton* serendipitous survey (Watson et al. 2009; Webb et al. 2020), the *Swift*/XRT point-source catalog (2SXPS; Evans et al. 2020), and the *Chandra* source catalog 2.0 (Evans et al. 2010). Specifically, we searched for soft X-ray counterparts within $5'$ of the positions of the *INTEGRAL* sources and only considered sources with a significant detection above 2 keV and the corresponding X-ray flux $F_X \gtrsim 10^{-13}$ erg s^{-1} cm^{-2}. We then searched for a positionally coincident optical or radio source using the VizieR (Ochsenbein et al. 2000) service, in order to determine the source class. As a result, we have found soft X-ray counterparts for 8 out of the 46 new *INTEGRAL* sources and classified some of these objects (see Table 6). Most of them are likely of extragalactic nature.

The identification completeness of the survey, i.e. the fraction of identified sources, is $(N_{\text{Tot}} - N_{\text{NotID}})/N_{\text{Tot}} = 1 - 113/929 \sim 0.88$. Interestingly, it is the same for both the Galactic ($|b| < 5°$) and

extragalactic ($|b| > 5°$) parts of the sky. As expected, due to the continuously increasing depth of the *INTEGRAL* all-sky survey, the fraction of identified sources sources has decreased compared to our previous compilation of the all-sky catalog, where it was 93% and 96% at $|b| < 5°$ and $|b| > 5°$, respectively (Krivonos et al. 2010b).

Most of the *INTEGRAL* sources in the current survey have X-ray counterparts in the *Swift*/BAT 70- and 105-month catalogs (Baum-

Table 6. Soft X-ray ($E > 2$ keV) counterparts of *INTEGRAL* sources discovered in the hard X-ray ($17 - 60$ keV) band.

Name	X-ray	Offset	Type	Notes
IGR J04085-6546	2RXS J040840.0-654545, XMMSL2 J040839.1-654600	0.3′	AGN	LEDA 310383, z=0.125 (Spiro et al. 2013)
IGR J07328-4640	2RXS J073245.8-464006, 4XMM J073244.3-464017	1.4′	BLAZAR?	PKS 0731-465
IGR J10595-5125	2RXS J105920.3-512644, 2SXPS J105918.9-512632	2.3′	SEYFERT	ESO 215-14, z=0.019
IGR J16005-4645	2RXS J160019.6-464802, 2SXPS J160020.4-464841	3.6′	AGN?	Edelson & Malkan (2012)
IGR J17227+3411	4XMM J172230.8+341339, 2SXPS J172230.9+341341	3.5′	AGN?	z=0.425 (Caccianiga et al. 2008)
IGR J17342-4049	XMMSL2 J173425.6-405121	2.2′		
IGR J17449-3037	4XMM J174507.9-303905	3.4′		
IGR J18006-3426	2SXPS J180050.6-342322	4.1′		

gartner et al. 2013; Oh et al. 2018, respectively). Taking the different sky coverage by *INTEGRAL*/IBIS and *Swift*/BAT into account, it is interesting to investigate the properties of the *INTEGRAL* sources that are not present in the *Swift*/BAT catalogs. According to Table 2, 711 *INTEGRAL* sources have counterparts in the *Swift*/BAT 105-month survey and 218 (929-711) sources are missed. The majority of the unmatched *INTEGRAL* sources (165 out of 218) prove to be located near the Galactic plane at $|b| < 17.5°$, which is the characteristic latitude span of the *INTEGRAL* Galactic surveys (Krivonos et al. 2012). This indicates that the *INTEGRAL*/IBIS survey has higher sensitivity near the Galactic plane compared to the *Swift*/BAT surveys. Similar evidence has been demonstrated by Bird et al. (2016) in comparing their *INTEGRAL* catalog with the *Swift*/BAT 70-month survey by Baumgartner et al. (2013). Among the 53 *INTEGRAL* sources at $|b| > 17.5°$ that are absent in the *Swift*/BAT 105-month catalog there are 5 HMXBs, 11 non-blazar AGN, 4 blazars, 32 unidentified objects, and the supernova AT2018cow; 17 are newly discovered sources in hard X-ray domain (see Sect. 2.3).

Bird et al. (2016) (hereafter B16) presented a hard X-ray source catalog based on *INTEGRAL*/IBIS observations performed in the first 1000 orbits of *INTEGRAL* (up to the end of 2010). This catalog includes 939 sources detected in the 17–100 keV band above a 4.5σ significance threshold. The final catalog was constructed using the "burstcity" method, based on finding the time window wherein the significance of detection of a given source is highest. As a result, 342 sources (out of 939) are transients found on different timescales, labeled with a variability flag in the B16 catalog. We have cross-correlated our source list with the B16 catalog and found 643 matches within a 10′ radius. Among them, 140 sources are marked with a 'Y' flag by B16, which implies moderate variability, and 12 are strongly variable sources, labeled as 'YY'. The remaining 491 sources are not labeled as variable in the B16 catalog. Therefore, the majority (76%) of our 643 sources that have matches in the B16 catalog are presumed to be persistent ones, whereas the ~300 B16 sources that are not confirmed by the present survey are mainly transients detected on *INTEGRAL*/IBIS sky maps of various timescales and not present on the all-time maps (see B16 for details). However, ~100 persistent B16 sources have not been found in our catalog either. These sources are characterized by sub-mCrab fluxes and have a median detection significance ~6σ, i.e. they were found close to the detection threshold in the B16 survey. Possible explanations for their absence in the present catalog may lie in the different data analysis methods and slightly different energy bands, substantial source variability, and some of the weak B16 sources being false detections. Because B16 is the most recent previous *INTEGRAL*/IBIS all-sky survey, we added

a special flag for all 286 new sources in our catalog that were not detected by B16.

4.2 Extragalactic LogN–LogS

Assuming that AGNs are uniformly distributed over the sky, we can construct their number–flux function in the hard X-ray band. As *INTEGRAL* observations cover the sky inhomogeneously, we must take the sensitivity map into account. To this end, we divided the observed source counts by the sky coverage at the 4.5σ level as a function of flux (Fig. 1). Figure 2 shows the resulting cumulative Log$N$-Log$S$ distribution based on the 356 non-blazar AGNs detected at $S/N > 4.5\sigma$ over the whole sky. AGN Log$N$-Log$S$ distributions are usually approximated by a power law $N(> S) = AS^{-\alpha}$. Using a maximum-likelihood estimator (Jauncey 1967; Crawford et al. 1970), we determined the best-fit value of the slope $\alpha = 1.44\pm0.09$ using the source counts at fluxes above 10^{-11} erg s^{-1} cm^{-2}, where our source sample is expected to be highly complete. We fixed the normalization of the power law at the observed value of the Log$N$-Log$S$ distribution at $S = 10^{-11}$ erg s^{-1} cm^{-2}, $A = 8 \times 10^{-3}$ deg^{-2}. The inferred Log$N$-Log$S$ slope α is consistent with a homogeneous distribution of sources in space ($\alpha = 3/2$).

At fluxes below ~5×10^{-12} erg s^{-1} cm^{-2}, the measured Log$N$-Log$S$ demonstrates a significant deficit of observed source counts relative to the aforementioned power-law dependence. This occurs far above both the known flattening of AGN number counts (in the 2–10 keV energy band) at ~10^{-14} erg s^{-1} cm^{-2} (Georgakakis et al. 2008) and the upturn at fluxes below ~2×10^{-13} erg s^{-1} cm^{-2} observed between the *NuSTAR* and *Swift*/BAT number-flux relations (Ajello et al. 2012; Harrison et al. 2016; Akylas & Georgantopoulos 2019, see also below). Thus, no deviations from the canonical $\alpha = 3/2$ are expected at fluxes $\lesssim 10^{-11}$erg s^{-1} cm^{-2}, and the observed slope flattening is likely caused by incompleteness of the source sample. To check this, we constructed an all-sky Log$N$-Log$S$ relation for the 104 unclassified sources at $S/N > 4.5\sigma$, which is shown in Fig. 2. This Log$N$-Log$S$ is well approximated with a power law and characterized by a steep $\alpha = 2.8 \pm 0.2$ and normalization $A = 4.9 \times 10^{-3}$ deg^{-2} at $S = 5 \times 10^{-12}$erg s^{-1} cm^{-2}. It turns out that the combined Log$N$-Log$S$ distribution of unidentified sources and non-blazar AGNs follows a power law with $\alpha \sim 3/2$ ($\alpha = 1.40 \pm 0.05$; $A = 8.7 \times 10^{-3}$ deg^{-2} at $S = 10^{-11}$ erg s^{-1} cm^{-2}; calculated over the whole range of fluxes), as demonstrated in Fig. 2. This suggests that the majority of the unidentified sources are of extragalactic origin.

Over the past two decades, number counts of extragalactic objects in hard X-ray domain have been independently measured with *INTEGRAL*/IBIS (e.g., Krivonos et al. 2005, 2007b, 2015; Beck-
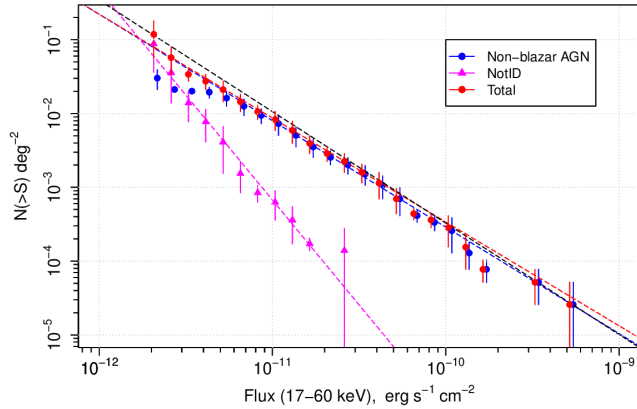
Figure 2. Binned number-flux relation for the 356 non-blazar AGNs (Seyferts and unclassified AGNs, blue points), 104 unidentified sources (magenta triangles), and 460 objects in total (red points) detected above the 4.5σ detection level. The binning of the blue and red points is slightly shifted for better visibility. The best-fitting power laws for the non-blazar AGNs and unidentified sources are shown by the dashed lines in the corresponding colors. For comparison, the dashed black line shows the AGN number-flux relation from Akylas & Georgantopoulos (2019) based on the *Swift*/BAT 105-months source catalog (Oh et al. 2018).

mann et al. 2006; Bazzano et al. 2006) and *Swift*/BAT (e.g., Tueller et al. 2008; Ajello et al. 2012). Krivonos et al. (2010c) compared the AGN Log$N$-Log$S$ distribution determined with *INTEGRAL*/IBIS in the 17–60 keV band with the one derived in the 15–55 keV band from the *Swift*/BAT AGN sample by Ajello et al. (2009) and found an excellent agreement (see also Cusumano et al. 2010). On the other hand, Harrison et al. (2016) presented *NuSTAR* 8–24 keV AGN number counts at lower fluxes that lay significantly above a simple extrapolation with a Euclidean slope of the *Swift*/BAT counts. However, Akylas & Georgantopoulos (2019) demonstrated that the bright part of the *NuSTAR* AGN number counts was in agreement with the *Swift*/BAT counts.

In light of the updated *INTEGRAL* AGN number counts, we compare them in Fig. 2 with the *Swift*/BAT 105-month AGN Log$N$-Log$S$ modelled by Akylas & Georgantopoulos (2019). To this end, we converted the 14–195 keV *Swift*/BAT number counts to the 17–60 keV band following Krivonos et al. (2010c). As seen from Fig. 2, the *Swift*/BAT Log$N$-Log$S$ has a slope ($\alpha = 1.51 \pm 0.10$, Akylas & Georgantopoulos 2019), which is better consistent with the canonical $\alpha = 3/2$ value than the slope obtained in the present work but is consistent with the latter as well. The small difference between *Swift*/BAT and *INTEGRAL*/IBIS may be partially caused by the fact that Akylas & Georgantopoulos (2019) included beamed AGNs in their counts while we tried to select only non-blazar AGN (although some blazars may be present among our unclassified AGN and unidentified sources). Nevertheless, our Log$N$-Log$S$ tends to be even less compatible with the *NuSTAR* number counts than *Swift*/BAT.

Finally, we plan to maintain an extended online version of the *INTEGRAL*/IBIS 17-year hard X-ray source catalog at `http://integral.cosmos.ru` where additional information will be presented. Specifically, we plan to provide soft X-ray and optical coordinates (where available), spectral information, and multi-year light curves of the detected sources, as well as sky images in different energy bands up to 290 keV.

DATA AVAILABILITY

This work is based on publicly available data of the *INTEGRAL* observatory. The ISDC Data Centre for Astrophysics (`http://isdc.unige.ch/`) provides the scientific archive of the *INTEGRAL* data to the community.

REFERENCES

Acero F., et al., 2015, ApJS, 218, 23
Aharonian F., et al., 2005, A&A, 442, 1
Ajello M., et al., 2009, ApJ, 699, 603
Ajello M., Alexander D. M., Greiner J., Madejski G. M., Gehrels N., Burlon D., 2012, ApJ, 749, 21
Akylas A., Georgantopoulos I., 2019, A&A, 625, A131
Altamirano D., et al., 2008, The Astronomer's Telegram, 1651, 1
Apparao K. M. V., Bignami G. F., Maraschi L., Helmken H., Margon B., Hjellming R., Bradt H. V., Dower R. G., 1978, Nature, 273, 450
Armas Padilla M., Muñoz-Darias T., Sánchez-Sierras J., De Marco B., Jiménez-Ibarra F., Casares J., Corral-Santana J. M., Torres M. A. P., 2019, MNRAS, 485, 5235
Bahramian A., Gladstone J. C., Heinke C. O., Wijnands R., Kaur R., Altamirano D., 2014, MNRAS, 441, 640
Barlow E. J., et al., 2005, A&A, 437, L27
Barlow E. J., Knigge C., Bird A. J., J Dean A., Clark D. J., Hill A. B., Molina M., Sguera V., 2006, MNRAS, 372, 224
Barthelmy S. D., et al., 2005, Space Sci. Rev., 120, 143
Barthelmy S. D., et al., 2019, The Astronomer's Telegram, 12436, 1
Bassani L., et al., 2004, The Astronomer's Telegram, 232, 1
Bassani L., et al., 2005, ApJ, 634, L21
Bassani L., et al., 2006, ApJ, 636, L65
Bassani L., et al., 2007, ApJ, 669, L1
Bassani L., et al., 2009, MNRAS, 395, L1
Bassani L., Landi R., Malizia A., Stephen J. B., Bazzano A., Bird A. J., Ubertini P., 2014, A&A, 561, A108
Bassi T., et al., 2019, MNRAS, 482, 1587
Baumgartner W. H., Tueller J., Markwardt C., Skinner G., 2010, in AAS/High Energy Astrophysics Division #11. p. 13.05

Baumgartner W. H., Tueller J., Markwardt C. B., Skinner G. K., Barthelmy S., Mushotzky R. F., Evans P. A., Gehrels N., 2013, ApJS, 207, 19

Bazzano A., et al., 2006, ApJ, 649, L9

Beckmann V., et al., 2005, ApJ, 631, 506

Beckmann V., Soldi S., Shrader C. R., Gehrels N., Produit N., 2006, ApJ, 652, 126

Bélanger G., et al., 2006, ApJ, 636, 275

Beri A., et al., 2021, MNRAS, 500, 565

Bernardini F., de Martino D., Falanga M., Mukai K., Matt G., Bonnet-Bidaud J. M., Masetti N., Mouchet M., 2012, A&A, 542, A22

Bernardini F., de Martino D., Mukai K., Israel G., Falanga M., Ramsay G., Masetti N., 2015, MNRAS, 453, 3100

Bernardini F., de Martino D., Mukai K., Falanga M., 2018, MNRAS, 478, 1185

Bikmaev I. F., Sunyaev R. A., Revnivtsev M. G., Burenin R. A., 2006, Astronomy Letters, 32, 221

Bikmaev I. F., Burenin R. A., Revnivtsev M. G., Sazonov S. Y., Sunyaev R. A., Pavlinsky M. N., Sakhibullin N. A., 2008a, Astronomy Letters, 34, 653

Bikmaev I., Revnivtsev M., Burenin R., Sazonov S., Sunyaev R., Pavlinsky M., Galeev A., Sakhibullin N., 2008b, The Astronomer's Telegram, 1363, 1

Bikmaev I., et al., 2017, The Astronomer's Telegram, 10968, 1

Bird A. J., et al., 2004, ApJ, 607, L33

Bird A. J., et al., 2006, ApJ, 636, 765

Bird A. J., et al., 2007, ApJS, 170, 175

Bird A. J., et al., 2010, ApJS, 186, 1

Bird A. J., et al., 2016, ApJS, 223, 15

Bodaghee A., Walter R., Zurita Heras J. A., Bird A. J., Courvoisier T. J. L., Malizia A., Terrier R., Ubertini P., 2006, A&A, 447, 1027

Bodaghee A., Tomsick J. A., Rodriguez J., 2012, ApJ, 753, 3

Bordas P., et al., 2010, The Astronomer's Telegram, 2919, 1

Bozzo E., Beardmore A., Papitto A., Ferrigno C., Gibaud L., 2011, The Astronomer's Telegram, 3558, 1

Bozzo E., Romano P., Falanga M., Ferrigno C., Papitto A., Krimm H. A., 2015, A&A, 579, A56

Bozzo E., et al., 2018a, A&A, 613, A22

Bozzo E., Savchenko V., Ferrigno C., Ducci L., Kuulkers E., Ubertini P., Laurent P., 2018b, The Astronomer's Telegram, 11478, 1

Brandt S., Budtz-Jørgensen C., Chenevez J., 2006a, The Astronomer's Telegram, 778, 1

Brandt S., Budtz-Jorgensen C., Chenevez J., Lund N., Oxborrow C. A., Westergaard N. J., 2006b, The Astronomer's Telegram, 970, 1

Brandt S., Budtz-Jørgensen C., Gotz D., Hurley K., Frontera F., 2007, The Astronomer's Telegram, 1054, 1

Brandt S., et al., 2008, The Astronomer's Telegram, 1400, 1

Britt C. T., et al., 2013, ApJ, 769, 120

Burenin R., Mescheryakov A., Revnivtsev M., Bikmaev I., Sunyaev R., 2006a, The Astronomer's Telegram, 880, 1

Burenin R., Mescheryakov A., Sazonov S., Revnivtsev M., Bikmaev I., Sunyaev R., 2006b, The Astronomer's Telegram, 883, 1

Burenin R., Revnivtsev M., Mescheryakov A., Bikmaev I., Pavlinsky M., Sunyaev R., 2007, The Astronomer's Telegram, 1270, 1

Burenin R. A., Mescheryakov A. V., Revnivtsev M. G., Sazonov S. Y., Bikmaev I. F., Pavlinsky M. N., Sunyaev R. A., 2008, Astronomy Letters, 34, 367

Burenin R., Makarov D., Uklein R., Revnivtsev M., Lutovinov A., 2009, The Astronomer's Telegram, 2193, 1

Butler S. C., et al., 2009, ApJ, 698, 502

Caballero I., et al., 2013, arXiv e-prints, p. arXiv:1304.1349

Caccianiga A., et al., 2008, A&A, 477, 735

Capitanio F., et al., 2006, ApJ, 643, 376

Chakrabarty D., Jonker P., Markwardt C. B., 2011a, The Astronomer's Telegram, 3218, 1

Chakrabarty D., Markwardt C. B., Linares M., Jonker P. G., 2011b, The Astronomer's Telegram, 3606, 1

Chaty S., Rahoui F., Foellmi C., Tomsick J. A., Rodriguez J., Walter R., 2008, A&A, 484, 783

Chelovekov I. V., Grebenev S. A., 2007, Astronomy Letters, 33, 807

Chenevez J., et al., 2012, The Astronomer's Telegram, 4050, 1

Chernyakova M., Lutovinov A., Capitano F., Lund N., Gehrels N., 2003, The Astronomer's Telegram, 157, 1

Chernyakova M., Lutovinov A., Rodríguez J., Revnivtsev M., 2005, MNRAS, 364, 455

Churazov E., et al., 2007, A&A, 467, 529

Churazov E., et al., 2014, Nature, 512, 406

Clavel M., et al., 2016, MNRAS, 461, 304

Clavel M., Tomsick J. A., Hare J., Krivonos R., Mori K., Stern D., 2019, ApJ, 887, 32

Cocchi M., Bazzano A., Natalucci L., Ubertini P., Heise J., Muller J. M., in 't Zand J. J. M., 1999, A&A, 346, L45

Coe M. J., Bartlett E. S., Bird A. J., Haberl F., Kennea J. A., McBride V. A., Townsend L. J., Udalski A., 2015, MNRAS, 447, 2387

Coleiro A., Chaty S., Zurita Heras J. A., Rahoui F., Tomsick J. A., 2013, A&A, 560, A108

Cornelisse R., Verbunt F., in't Zand J. J. M., Kuulkers E., Heise J., 2002, A&A, 392, 931

Courvoisier T. J. L., Walter R., Rodriguez J., Bouchet L., Lutovinov A. A., 2003, IAU Circ., 8063, 3

Crawford D. F., Jauncey D. L., Murdoch H. S., 1970, ApJ, 162, 405

Curran P. A., Chaty S., Zurita Heras J. A., 2011, A&A, 533, A3

Cusumano G., et al., 2010, A&A, 510, A48

Cusumano G., D'Aì A., Segreto A., La Parola V., Del Santo M., 2020, MNRAS, 498, 2750

D'Aì A., La Parola V., Cusumano G., Segreto A., Romano P., Vercellone S., Robba N. R., 2011, A&A, 529, A30

Degenaar N., et al., 2007, The Astronomer's Telegram, 1136, 1

Degenaar N., et al., 2010, MNRAS, 404, 1591

Degenaar N., Yang Y. J., Wijnands R., 2011, The Astronomer's Telegram, 3741, 1

Degenaar N., Altamirano D., Wijnands R., 2012, The Astronomer's Telegram, 4219, 1

Del Monte E., et al., 2008a, in The 7th INTEGRAL Workshop. p. 122

Del Monte E., et al., 2008b, The Astronomer's Telegram, 1445, 1

Del Santo M., et al., 2011, The Astronomer's Telegram, 3210, 1

Del Santo M., Nucita A. A., Lodato G., Manni L., De Paolis F., Farihi J., De Cesare G., Segreto A., 2014, MNRAS, 444, 93

Del Santo M., et al., 2016, MNRAS, 456, 3585

Doroshenko V., et al., 2020a, MNRAS, 491, 1857

Doroshenko V., Tsygankov S., Long J., Santangelo A., Molkov S., Lutovinov A., Kong L. D., Zhang S., 2020b, A&A, 634, A89

Ducci L., Kuulkers E., Grinberg V., Paizis A., Sidoli L., Bozzo E., Ferrigno C., Savchenko V., 2018, The Astronomer's Telegram, 11941, 1

Eckert D., Walter R., Kretschmar P., Mas-Hesse M., Palumbo G. G. C., Roques J. P., Ubertini P., Winkler C., 2004, The Astronomer's Telegram, 352, 1

Eckert D., et al., 2013, The Astronomer's Telegram, 4925, 1

Edelson R., Malkan M., 2012, ApJ, 751, 52

Esposito P., Israel G. L., Sidoli L., Mason E., Rodríguez Castillo G. A., Halpern J. P., Moretti A., Götz D., 2013, MNRAS, 433, 2028

Evans I. N., et al., 2010, ApJS, 189, 37

Evans P. A., et al., 2020, ApJS, 247, 54

Falanga M., Bozzo E., Walter R., Sarty G. E., Stella L., 2011, Journal of the American Association of Variable Star Observers (JAAVSO), 39, 110

Ferrigno C., Bozzo E., Belloni L. G. A. P. T. M., 2011, The Astronomer's Telegram, 3560, 1

Ferrigno C., Bozzo E., Del Santo M., Capitano F., 2012, A&A, 537, L7

Fiocchi M., Bassani L., Bazzano A., Ubertini P., Landi R., Capitanio F., Bird A. J., 2010, ApJ, 720, 987

Fornasini F. M., Tomsick J. A., Bachetti M., Krivonos R. A., Fürst F., Natalucci L., Pottschmidt K., Wilms J., 2017, ApJ, 841, 35

Fortin F., Chaty S., Coleiro A., Tomsick J. A., Nitschelm C. H. R., 2018, A&A, 618, A150

Fuerst F., et al., 2018, The Astronomer's Telegram, 11357, 1

Funk S., et al., 2007, A&A, 470, 249

Gänsicke B. T., et al., 2005, MNRAS, 361, 141

Gehrels N., et al., 2004, ApJ, 611, 1005

Georgakakis A., Nandra K., Laird E. S., Aird J., Trichas M., 2008, MNRAS, 388, 1205

Gianní S., de Rosa A., Bassani L., Bazzano A., Dean T., Ubertini P., 2011, MNRAS, 411, 2137

Gibaud L., et al., 2011, The Astronomer's Telegram, 3565, 1

Goncalves T. S., Martin D. C., Halpern J. P., Eracleous M., Pavlov G. G., 2008, The Astronomer's Telegram, 1623, 1

González-Martín O., et al., 2011, A&A, 527, A142

Goossens M. E., Bird A. J., Hill A. B., Sguera V., Drave S. P., 2019, MNRAS, 485, 286

Górski K. M., Hivon E., Banday A. J., Wandelt B. D., Hansen F. K., Reinecke M., Bartelmann M., 2005, ApJ, 622, 759

Grebenev S. A., Sunyaev R. A., 2004, The Astronomer's Telegram, 342, 1

Grebenev S. A., Sunyaev R. A., 2007, Astronomy Letters, 33, 149

Grebenev S. A., Sunyaev R. A., 2010, Astronomy Letters, 36, 533

Grebenev S. A., Ubertini P., Chenevez J., Orr A., Sunyaev R. A., 2004, The Astronomer's Telegram, 275, 1

Grebenev S. A., Molkov S. V., Sunyaev R. A., 2005a, The Astronomer's Telegram, 444, 1

Grebenev S. A., Bird A. J., Molkov S. V., Soldi S., Kretschmar P., Diehl R., Budz-Joergensen C., McBreen B., 2005b, The Astronomer's Telegram, 457, 1

Grebenev S. A., Molkov S. V., Sunyaev R. A., 2005c, The Astronomer's Telegram, 467, 1

Grebenev S. A., Molkov S. V., Revnivtsev M. G., Sunyaev R. A., 2007a, in The Obscured Universe. Proceedings of the VI INTEGRAL Workshop. p. 3730376 (arXiv:0709.2313)

Grebenev S. A., Revnivtsev M. G., Sunyaev R. A., 2007b, The Astronomer's Telegram, 1319, 1

Grebenev S. A., Lutovinov A. A., Tsygankov S. S., Mereminskiy I. A., 2013, MNRAS, 428, 50

Grebenev S. A., Mereminskiy I. A., Prosvetov A. V., Ducci L., Bozzo E., Savchenko V., Ferrigno C., 2018, The Astronomer's Telegram, 11306, 1

Grebenev S. A., Mereminsky I. A., Bozzo E., Ferrigno C., Savchenko V., Ducci L., 2019, The Astronomer's Telegram, 13155, 1

Greiss S., Steeghs D., Maccarone T., Jonker P. G., Torres M. A. P., Gonzalez O., Masetti N., Rojas A., 2011, The Astronomer's Telegram, 3562, 1

Gros A., Goldwurm A., Cadolle-Bel M., Goldoni P., Rodriguez J., Foschini L., Del Santo M., Blay P., 2003, A&A, 411, L179

Halpern J. P., 2006, The Astronomer's Telegram, 847, 1

Halpern J. P., Gotthelf E. V., 2008, The Astronomer's Telegram, 1457, 1

Halpern J. P., Thorstensen J. R., 2018, The Astronomer's Telegram, 11787, 1

Halpern J. P., Tyagi S., 2005, The Astronomer's Telegram, 681, 1

Halpern J. P., Thorstensen J. R., Cho P., Collver G., Motsoaledi M., Breytenbach H., Buckley D. A. H., Woudt P. A., 2018, AJ, 155, 247

Hannikainen D. C., Rodriguez J., Pottschmidt K., 2003, IAU Circ., 8088, 4

Hare J., Halpern J. P., Clavel M., Grindlay J. E., Rahoui F., Tomsick J. A., 2019, ApJ, 878, 15

Hare J., Halpern J. P., Tomsick J. A., Thorstensen J. R., Bodaghee A., Clavel M., Krivonos R., Mori K., 2021, ApJ, 914, 85

Harrison F. A., et al., 2016, ApJ, 831, 185

Heinke C. O., Tomsick J. A., Yusef-Zadeh F., Grindlay J. E., 2009, ApJ, 701, 1627

Heinke C. O., et al., 2019, The Astronomer's Telegram, 12843, 1

Hiemstra B., Méndez M., Done C., Díaz Trigo M., Altamirano D., Casella P., 2011, MNRAS, 411, 137

Huchra J. P., et al., 2012, ApJS, 199, 26

Jauncey D. L., 1967, Nature, 216, 877

Kaaret P., Morgan E. H., Vanderspek R., Tomsick J. A., 2006, ApJ, 638, 963

Kalamkar M., Homan J., Altamirano D., van der Klis M., Casella P., Linares M., 2011, ApJ, 731, L2

Kalemci E., Tomsick J. A., Rothschild R. E., Pottschmidt K., Corbel S., Kaaret P., 2006, ApJ, 639, 340

Karasev D. I., Lutovinov A. A., Grebenev S. A., 2007, Astronomy Letters, 33, 159

Karasev D. I., Lutovinov A. A., Burenin R. A., 2008, Astronomy Letters, 34, 753

Karasev D. I., Lutovinov A. A., Burenin R. A., 2010, MNRAS, 409, L69

Karasev D. I., Lutovinov A. A., Revnivtsev M. G., Krivonos R. A., 2012, Astronomy Letters, 38, 629

Karasev D. I., et al., 2018, Astronomy Letters, 44, 522

Karasev D. I., et al., 2020, Astronomy Letters, 45, 836

Kaur R., Wijnands R., Paul B., Patruno A., Degenaar N., 2010, MNRAS, 402, 2388

Kaur R., Kotulla R., Degenaar N., Wijnands R., Kaplan D., 2011, The Astronomer's Telegram, 3268, 1

Kaur R., Wijnands R., Kamble A., Cackett E. M., Kutulla R., Kaplan D., Degenaar N., 2017, MNRAS, 464, 170

Keek S., Kuiper L., Hermsen W., 2006, The Astronomer's Telegram, 810, 1

Kennea J. A., et al., 2019, The Astronomer's Telegram, 13195, 1

Kniazev A., Revnivtsev M., Burenin R., Tkachenko A., 2010, The Astronomer's Telegram, 2457, 1

Koss M., Mushotzky R., Veilleux S., Winter L. M., Baumgartner W., Tueller J., Gehrels N., Valencic L., 2011, ApJ, 739, 57

Koss M., et al., 2017, ApJ, 850, 74

Kretschmar P., Mereghetti S., Hermsen W., Ubertini P., Winkler C., Brandt S., Diehl R., 2004, The Astronomer's Telegram, 345, 1

Kretschmar P., et al., 2019, New Astron. Rev., 86, 101546

Krimm H. A., Tomsick J. A., Markwardt C. B., Brocksopp C., Grisé F., Kaaret P., Romano P., 2011, ApJ, 735, 104

Krimm H. A., et al., 2012, The Astronomer's Telegram, 4130, 1

Krimm H. A., et al., 2013a, ApJS, 209, 14

Krimm H. A., et al., 2013b, The Astronomer's Telegram, 4769, 1

Krivonos R., Vikhlinin A., Churazov E., Lutovinov A., Molkov S., Sunyaev R., 2005, ApJ, 625, 89

Krivonos R., Revnivtsev M., Churazov E., Sazonov S., Grebenev S., Sunyaev R., 2007a, A&A, 463, 957

Krivonos R., Revnivtsev M., Lutovinov A., Sazonov S., Churazov E., Sunyaev R., 2007b, A&A, 475, 775

Krivonos R., Revnivtsev M., Lutovinov A., Sazonov S., Churazov E., Sunyaev R., 2007c, A&A, 475, 775

Krivonos R., Tsygankov S., Sunyaev R., Melnikov S., Bikmaev I., Pavlinsky M., Burenin R., 2009, The Astronomer's Telegram, 2170, 1

Krivonos R., Revnivtsev M., Tsygankov S., Sazonov S., Vikhlinin A., Pavlinsky M., Churazov E., Sunyaev R., 2010a, A&A, 519, A107

Krivonos R., Tsygankov S., Revnivtsev M., Grebenev S., Churazov E., Sunyaev R., 2010b, A&A, 523, A61

Krivonos R., Tsygankov S., Revnivtsev M., Grebenev S., Churazov E., Sunyaev R., 2010c, A&A, 523, A61

Krivonos R., Tsygankov S., Burenin R., Revnivtsev M., Lutovinov A., 2011, The Astronomer's Telegram, 3382, 1

Krivonos R., Tsygankov S., Lutovinov A., Revnivtsev M., Churazov E., Sunyaev R., 2012, A&A, 545, A27

Krivonos R., Lutovinov A., Molkov S., Revnivtsev M., Tsygankov S., Sunyaev R., 2013, The Astronomer's Telegram, 4924, 1

Krivonos R., Tsygankov S., Lutovinov A., Revnivtsev M., Churazov E., Sunyaev R., 2015, MNRAS, 448, 3766

Krivonos R. A., Tsygankov S. S., Mereminskiy I. A., Lutovinov A. A., Sazonov S. Y., Sunyaev R. A., 2017, MNRAS, 470, 512

Krivonos R., Sazonov S., Tsygankov S. S., Poutanen J., 2018, MNRAS, 480, 2357

Krivonos R. A., et al., 2021, New Astron. Rev., 92, 101612

Kuiper L., Hermsen W., 2009, A&A, 501, 1031

Kuiper L., Hermsen W., in't Zand J., den Hartog P. R., 2005, The Astronomer's Telegram, 662, 1

Kuiper L., Keek S., Hermsen W., Jonker P. G., Steeghs D., 2006a, The Astronomer's Telegram, 684, 1

Kuiper L., den Hartog P. R., Hermsen W., 2006b, The Astronomer's Telegram, 939, 1

Kuiper L., Jonker P. G., Torres M. A. P., Rest A., Keek S., 2008, The Astronomer's Telegram, 1774, 1

Kuulkers E., Lutovinov A., Parmar A., Capitanio F., Mowlavi N., Hermsen W., 2003, The Astronomer's Telegram, 149, 1

Kuulkers E., et al., 2006, The Astronomer's Telegram, 874, 1

Kuulkers E., et al., 2013, The Astronomer's Telegram, 4804, 1

Kuznetsova E., Krivonos R., Churazov E., Lyskova N., Lutovinov A., 2019, MNRAS, 489, 1828

Kuznetsova E., Krivonos R., Lutovinov A., Clavel M., 2022, MNRAS, 509, 1605

La Parola V., Cusumano G., Segreto A., D'Aì A., Masetti N., D'Elia V., 2013, ApJ, 775, L24

Lamperti I., et al., 2017, MNRAS, 467, 540

Landi R., et al., 2007, The Astronomer's Telegram, 1288, 1

Landi R., et al., 2009, A&A, 493, 893

Landi R., Bassani L., Malizia A., Stephen J. B., Bazzano A., Fiocchi M., Bird A. J., 2010a, MNRAS, 403, 945

Landi R., et al., 2010b, The Astronomer's Telegram, 2853, 1

Landi R., Malizia A., Bazzano A., Fiocchi M., Bird A. J., Gehrels N., 2011a, The Astronomer's Telegram, 3184, 1

Landi R., Bassani L., Masetti N., Bazzano A., Bird A. J., 2011b, The Astronomer's Telegram, 3271, 1

Landi R., Bassani L., Masetti N., Bazzano A., Bird A. J., 2011c, The Astronomer's Telegram, 3272, 1

Landi R., Bassani L., Masetti N., Bazzano A., Tarana A., Bird A. J., 2012, The Astronomer's Telegram, 4233, 1

Landi R., et al., 2017, MNRAS, 470, 1107

Lebrun F., et al., 2003, A&A, 411, L141

Leyder J. C., Walter R., Rauw G., 2008, A&A, 477, L29

Lubiński P., Cadolle Bel M., von Kienlin A., Budtz-Jorgensen C., McBreen B., Kretschmar P., Hermsen W., Shtykovsky P., 2005, The Astronomer's Telegram, 469, 1

Lutovinov A. A., Revnivtsev M. G., 2003, Astronomy Letters, 29, 719

Lutovinov A., Shaw S., Foschini L., Paul J., 2003a, The Astronomer's Telegram, 154, 1

Lutovinov A., Walter R., Belanger G., Lund N., Grebenev S., Winkler C., 2003b, The Astronomer's Telegram, 155, 1

Lutovinov A., Cadolle Bel M., Belanger G., Goldwurm A., Budtz-Jorgensen C., Mowlavi N., Paul J., Orr A., 2004a, The Astronomer's Telegram, 328, 1

Lutovinov A., Rodrigues J., Budtz-Jorgensen C., Grebenev S., Winkler C., 2004b, The Astronomer's Telegram, 329, 1

Lutovinov A., Rodriguez J., Revnivtsev M., Shtykovskiy P., 2005a, A&A, 433, L41

Lutovinov A., Revnivtsev M., Gilfanov M., Shtykovskiy P., Molkov S., Sunyaev R., 2005b, A&A, 444, 821

Lutovinov A. A., Burenin R. A., Revnivtsev M. G., Suleimanov V. F., Tkachenko A. Y., 2010a, Astronomy Letters, 36, 904

Lutovinov A., Burenin R., Sazonov S., Revnivtsev M., Moiseev A., Dodonov S., 2010b, The Astronomer's Telegram, 2759, 1

Lutovinov A. A., Burenin R. A., Revnivtsev M. G., Bikmaev I. F., 2012, Astronomy Letters, 38, 1

Lutovinov A. A., Mironov A. I., Burenin R. A., Revnivtsev M. G., Tsygankov S. S., Pavlinsky M. N., Korobtsev I. V., Eselevich M. V., 2013, Astronomy Letters, 39, 513

Lutovinov A., Suleimanov V., Manuel Luna G. J., Sazonov S., de Martino D., Ducci L., Doroshenko V., Falanga M., 2020, New Astron. Rev., 91, 101547

Malizia A., et al., 2005, ApJ, 630, L157

Malizia A., et al., 2007, ApJ, 668, 81

Malizia A., Bassani L., Sguera V., Stephen J. B., Bazzano A., Fiocchi M., Bird A. J., 2010, MNRAS, 408, 975

Malizia A., Bassani L., Bazzano A., Bird A. J., Masetti N., Panessa F., Stephen J. B., Ubertini P., 2012, MNRAS, 426, 1750

Malizia A., Landi R., Molina M., Bassani L., Bazzano A., Bird A. J., Ubertini P., 2016, MNRAS, 460, 19

Malizia A., Bassani L., Sguera V., Bazzano A., Fiocchi M. T., Ubertini P., Bird A. J., 2017, The Astronomer's Telegram, 10411, 1

Malizia A., Sazonov S., Bassani L., Pian E., Beckmann V., Molina M., Mereminskiy I., Belanger G., 2020, New Astron. Rev., 90, 101545

Margutti R., et al., 2019, ApJ, 872, 18

Markwardt C. B., 2008, The Astronomer's Telegram, 1686, 1

Markwardt C. B., Swank J. H., Strohmayer T. E., 2004, The Astronomer's Telegram, 353, 1

Martí J., Paredes J. M., Bloom J. S., Casares J., Ribó M., Falco E. E., 2004, A&A, 413, 309

Maselli A., et al., 2013, ApJS, 206, 17

Masetti N., Palazzi E., Bassani L., Malizia A., Stephen J. B., 2004, A&A, 426, L41

Masetti N., et al., 2006a, A&A, 449, 1139

Masetti N., et al., 2006b, A&A, 455, 11

Masetti N., et al., 2006c, A&A, 459, 21

Masetti N., Bassani L., Dean A. J., Ubertini P., Walter R., 2006d, The Astronomer's Telegram, 715, 1

Masetti N., Morelli L., Palazzi E., Stephen J., Bazzano A., Dean A. J., Walter R., Minniti D., 2006e, The Astronomer's Telegram, 783, 1

Masetti N., Rigon E., Maiorano E., Cusumano G., Palazzi E., Orlandini M., Amati L., Frontera F., 2007a, A&A, 464, 277

Masetti N., et al., 2007b, A&A, 470, 331

Masetti N., et al., 2007c, The Astronomer's Telegram, 1034, 1

Masetti N., et al., 2008, A&A, 482, 113

Masetti N., et al., 2009, A&A, 495, 121

Masetti N., et al., 2010a, A&A, 511, A48

Masetti N., et al., 2010b, A&A, 519, A96

Masetti N., et al., 2012a, A&A, 538, A123

Masetti N., Nucita A. A., Parisi P., 2012b, A&A, 544, A114

Masetti N., Jimenez-Bailon E., Chavushyan V., Parisi P., Bazzano A., Landi R., Bird A. J., 2012c, The Astronomer's Telegram, 4248, 1

Masetti N., et al., 2013, A&A, 556, A120

McCollum B., Laine S., 2019, The Astronomer's Telegram, 13211, 1

Mereminskiy I. A., Krivonos R. A., Lutovinov A. A., Sazonov S. Y., Revnivtsev M. G., Sunyaev R. A., 2016, MNRAS, 459, 140

Mescheryakov A., Burenin R., Sazonov S., Revnivtsev M., Bikmaev I., Sunyaev R., 2006, The Astronomer's Telegram, 948, 1

Mescheryakov A., Burenin R., Sazonov S., Revnivtsev M., Bikmaev I., Pavlinsky M., Sunyaev R., 2009, The Astronomer's Telegram, 2132, 1

Milisavljevic D., Fesen R. A., Parrent J. T., Thorstensen J. R., 2011, The Astronomer's Telegram, 3146, 1

Miyasaka H., Tomsick J. A., Xu Y., Harrison F. A., 2018, The Astronomer's Telegram, 12340, 1

Molina M., Venturi T., Malizia A., Bassani L., Dallacasa D., Lal D. V., Bird A. J., Ubertini P., 2015, MNRAS, 451, 2370

Molkov S., Mowlavi N., Goldwurm A., Strong A., Lund N., Paul J., Oosterbroek T., 2003, The Astronomer's Telegram, 176, 1

Molkov S. V., Cherepashchuk A. M., Lutovinov A. A., Revnivtsev M. G., Postnov K. A., Sunyaev R. A., 2004, Astronomy Letters, 30, 534

Morelli L., Masetti N., Bassani L., Landi R., Malizia A., Bird A. J., Ubertini P., Galaz G., 2006, The Astronomer's Telegram, 785, 1

Morgan E., Swank J., Markwardt C., Gehrels N., 2005, The Astronomer's Telegram, 550, 1

Mori K., et al., 2015, ApJ, 814, 94

Nabizadeh A., Tsygankov S. S., Karasev D. I., Mönkkönen J., Lutovinov A. A., Nagirner D. I., Poutanen J., 2019, A&A, 622, A198

Nakahira S., et al., 2013, The Astronomer's Telegram, 5474, 1

Natalucci L., Fiocchi M., Bazzano A., Kuulkers E., Sanchez C., 2011, The Astronomer's Telegram, 3181, 1

Nebot Gómez-Morán A., Motch C., Pineau F. X., Carrera F. J., Pakull M. W., Riddick F., 2015, MNRAS, 452, 884

Negoro H., et al., 2018, The Astronomer's Telegram, 12254, 1

Negueruela I., Schurch M. P. E., 2007, A&A, 461, 631

Negueruela I., Smith D. M., Chaty S., 2005, The Astronomer's Telegram, 470, 1

Negueruela I., Torrejón J. M., McBride V., 2007, The Astronomer's Telegram, 1239, 1

Nespoli E., Fabregat J., Mennickent R. E., 2008a, A&A, 486, 911

Nespoli E., Fabregat J., Mennickent R. E., 2008b, The Astronomer's Telegram, 1396, 1

Nespoli E., Fabregat J., Mennickent R. E., 2010, A&A, 516, A94

Neustroev V. V., Veledina A., Poutanen J., Zharikov S. V., Tsygankov S. S., Sjoberg G., Kajava J. J. E., 2014, MNRAS, 445, 2424

Nucita A. A., Carpano S., Guainazzi M., 2007, A&A, 474, L1

Nucita A. A., De Paolis F., Saxton R., Read A. M., 2012, New Astron., 17, 589

Ochsenbein F., Bauer P., Marcout J., 2000, A&AS, 143, 23

Oda S., et al., 2019, PASJ, 71, 108

Oh K., Yi S. K., Schawinski K., Koss M., Trakhtenbrot B., Soto K., 2015, ApJS, 219, 1

Oh K., et al., 2018, ApJS, 235, 4

Paizis A., et al., 2007, ApJ, 657, L109

Papitto A., Ferrigno C., Bozzo E., Gibaud L., Burderi L., di Salvo T., Riggio A., 2011, The Astronomer's Telegram, 3556, 1

Parikh A. S., Russell T. D., Wijnands R., Miller-Jones J. C. A., Sivakoff G. R., Tetarenko A. J., 2019, ApJ, 878, L28

Parisi P., et al., 2008, The Astronomer's Telegram, 1540, 1

Parisi P., et al., 2012, The Astronomer's Telegram, 4151, 1

Parisi P., et al., 2014, A&A, 561, A67

Pavan L., Bozzo E., Ferrigno C., Ricci C., Manousakis A., Walter R., Stella L., 2011, A&A, 526, A122

Pavlinsky M. N., Grebenev S. A., Sunyaev R. A., 1994, ApJ, 425, 110

Pavlinsky M., et al., 2021, arXiv e-prints, p. arXiv:2107.05879

Pearlman A. B., Coley J. B., Corbet R. H. D., Pottschmidt K., 2019, ApJ, 873, 86

Produit N., Ballet J., Mowlavi N., 2004, The Astronomer's Telegram, 278, 1

Rahoui F., Tomsick J. A., Krivonos R., 2017, MNRAS, 465, 1563

Ratti E. M., Bassa C. G., Torres M. A. P., Kuiper L., Miller-Jones J. C. A., Jonker P. G., 2010, MNRAS, 408, 1866

Rau A., 2018, The Astronomer's Telegram, 11332, 1

Renaud M., et al., 2010, ApJ, 716, 663

Revnivtsev M. G., Sazonov S. Y., Gilfanov M. R., Sunyaev R. A., 2003a, Astronomy Letters, 29, 587

Revnivtsev M., Chernyakova M., Capitanio F., Westergaard N. J., Shoenfelder V., Gehrels N., Winkler C., 2003b, The Astronomer's Telegram, 132, 1

Revnivtsev M., Tuerler M., Del Santo M., Westergaard N. J., Gehrels N., Winkler C., 2003c, IAU Circ., 8097, 2

Revnivtsev M. G., et al., 2004a, Astronomy Letters, 30, 382

Revnivtsev M. G., et al., 2004b, A&A, 425, L49

Revnivtsev M. G., Sazonov S. Y., Molkov S. V., Lutovinov A. A., Churazov E. M., Sunyaev R. A., 2006, Astronomy Letters, 32, 145

Revnivtsev M., Sunyaev R., Lutovinov A., Sazonov S., 2007, The Astronomer's Telegram, 1253, 1

Revnivtsev M., Lutovinov A., Churazov E., Sazonov S., Gilfanov M., Grebenev S., Sunyaev R., 2008, A&A, 491, 209

Revnivtsev M. G., et al., 2009, Astronomy Letters, 35, 33

Reynolds M. T., et al., 2012, The Astronomer's Telegram, 3951, 1

Ricci C., et al., 2017, ApJS, 233, 17

Rodes-Roca J. J., Bernabeu G., Magazzù A., Torrejón J. M., Solano E., 2018, MNRAS, 476, 2110

Rodriguez J., et al., 2004, The Astronomer's Telegram, 340, 1

Rodriguez J., Cadolle Bel M., Tomsick J. A., Corbel S., Brocksopp C., Paizis A., Shaw S. E., Bodaghee A., 2007, ApJ, 655, L97

Rodriguez J., Tomsick J. A., Chaty S., 2008, A&A, 482, 731

Rodriguez J., Tomsick J. A., Chaty S., 2009, A&A, 494, 417

Rodriguez J., Tomsick J. A., Bodaghee A., 2010, A&A, 517, A14

Rojas A. F., et al., 2017, A&A, 602, A124

Russell D. M., Lewis F., Altamirano D., Roche P., 2011, The Astronomer's Telegram, 3622, 1

Russell T. D., et al., 2019, ApJ, 883, 198

Sanchez-Fernandez C., Eckert D., Bozzo E., Kajava J., Kuulkers E., Chenevez J., 2015, The Astronomer's Telegram, 7946, 1

Sanna A., et al., 2017, A&A, 598, A34

Sanna A., et al., 2018, A&A, 617, L8

Saxton R. D., Read A. M., Esquej P., Freyberg M. J., Altieri B., Bermejo D., 2008, A&A, 480, 611

Sazonov S., Churazov E., Revnivtsev M., Vikhlinin A., Sunyaev R., 2005, A&A, 444, L37

Sazonov S., Revnivtsev M., Krivonos R., Churazov E., Sunyaev R., 2007, A&A, 462, 57

Sazonov S., Revnivtsev M., Burenin R., Churazov E., Sunyaev R., Forman W. R., Murray S. S., 2008, A&A, 487, 509

Sazonov S., et al., 2020, New Astron. Rev., 88, 101536

Scott D. M., Finger M. H., Wilson R. B., Koh D. T., Prince T. A., Vaughan B. A., Chakrabarty D., 1997, ApJ, 488, 831

Segreto A., Cusumano G., La Parola V., D'Aì A., Masetti N., D'Avanzo P., 2013, A&A, 557, A113

Sguera V., Drave S. P., Sidoli L., Masetti N., Landi R., Bird A. J., Bazzano A., 2013, A&A, 556, A27

Sguera V., Sidoli L., Bird A. J., Paizis A., Bazzano A., 2020, MNRAS, 491, 4543

Shaw A. W., Heinke C. O., Degenaar N., Wijnands R., Kaur R., Forestell L. M., 2017, MNRAS, 471, 2508

Shidatsu M., et al., 2018, ApJ, 868, 54

Sidoli L., Paizis A., Mereghetti S., 2006, A&A, 450, L9

Sidoli L., Paizis A., Mereghetti S., Götz D., Del Santo M., 2011, MNRAS, 415, 2373

Smith N., Hartigan P., 2006, ApJ, 638, 1045

Soldi S., Brandt S., Garau A. D., Grebenev S. A., Kuulkers E., Palumbo G. G. C., Tarana A., 2005, The Astronomer's Telegram, 456, 1

Soldi S., et al., 2006, The Astronomer's Telegram, 885, 1

Spiro S., et al., 2013, The Astronomer's Telegram, 5537, 1

Steeghs D., Knigge C., Drew J., Unruh Y., Greimel R., 2008, The Astronomer's Telegram, 1653, 1

Stephen J. B., Bassani L., Malizia A., Masetti N., Ubertini P., 2018, The Astronomer's Telegram, 11341, 1

Sunyaev R., Lutovinov A., Molkov S., Deluit S., 2003a, The Astronomer's Telegram, 181, 1

Sunyaev R. A., Grebenev S. A., Lutovinov A. A., Rodriguez J., Mereghetti S., Gotz D., Courvoisier T., 2003b, The Astronomer's Telegram, 190, 1

Terrier R., Mattana F., Djannati-Atai A., Marandon V., Renaud M., Dubois F., 2008, in Aharonian F. A., Hofmann W., Rieger F., eds, American Institute of Physics Conference Series Vol. 1085, American Institute of Physics Conference Series. pp 312–315, doi:10.1063/1.3076669

Terrier R., et al., 2010, ApJ, 719, 143

Tomsick J. A., Lingenfelter R., Walter R., Rodriguez J., Goldwurm A., Corbel S., Kaaret P., 2003, IAU Circ., 8076, 1

Tomsick J. A., Lingenfelter R., Corbel S., Goldwurm A., Kaaret P., 2004, The Astronomer's Telegram, 224, 1

Tomsick J. A., Chaty S., Rodriguez J., Foschini L., Walter R., Kaaret P., 2006, ApJ, 647, 1309

Tomsick J. A., Chaty S., Rodriguez J., Walter R., Kaaret P., 2008, ApJ, 685, 1143

Tomsick J. A., Chaty S., Rodriguez J., Walter R., Kaaret P., 2009, ApJ, 701, 811

Tomsick J. A., Bodaghee A., Chaty S., Rodriguez J., Rahoui F., Halpern J., Kalemci E., Özbey Arabaci M., 2012, ApJ, 754, 145

Tomsick J. A., Krivonos R., Rahoui F., Ajello M., Rodriguez J., Barrière N., Bodaghee A., Chaty S., 2015, MNRAS, 449, 597

Tomsick J. A., Rahoui F., Krivonos R., Clavel M., Strader J., Chomiuk L., 2016a, MNRAS, 460, 513

Tomsick J. A., Krivonos R., Wang Q., Bodaghee A., Chaty S., Rahoui F., Rodriguez J., Fornasini F. M., 2016b, ApJ, 816, 38

Tomsick J. A., et al., 2020, ApJ, 889, 53

Tomsick J. A., et al., 2021, ApJ, 914, 48

Torrejón J. M., Negueruela I., Smith D. M., Harrison T. E., 2010, A&A, 510, A61

Torres M. A. P., Garcia M. R., McClintock J. E., Steeghs D., Miller J., Callanan P. J., Zhao P., Berlind P., 2004, The Astronomer's Telegram, 264, 1

Torres M. A. P., Steeghs D., Garcia M. R., McClintock J. E., Berlind P., Zhao P., Jonker P. G., Callanan P. J., 2006, The Astronomer's Telegram, 862, 1

Tovmassian G., et al., 2017, A&A, 608, A36

Townsend L. J., et al., 2011, MNRAS, 410, 1813

Tueller J., et al., 2005, The Astronomer's Telegram, 669, 1

Tueller J., Mushotzky R. F., Barthelmy S., Cannizzo J. K., Gehrels N., Markwardt C. B., Skinner G. K., Winter L. M., 2008, ApJ, 681, 113

Tueller J., et al., 2010, ApJS, 186, 378

Tuerler M., Walter R., Ferrigno C., 2012, The Astronomer's Telegram, 4183, 1

Ubertini P., et al., 2003, A&A, 411, L131

Ubertini P., et al., 2005, ApJ, 629, L109

Vasilopoulos G., Maggi P., Haberl F., Sturm R., Pietsch W., Bartlett E. S., Coe M. J., 2013, A&A, 558, A74

Vasilopoulos G., Haberl F., Sturm R., Maggi P., Udalski A., 2014, A&A, 567, A129

Voges W., et al., 1999, A&A, 349, 389

Vovk I., et al., 2012, The Astronomer's Telegram, 4381, 1

Walter R., et al., 2004, The Astronomer's Telegram, 229, 1

Walter R., et al., 2006, A&A, 453, 133

Wang W., 2010, A&A, 516, A15

Watson M. G., et al., 2009, A&A, 493, 339

Webb N. A., et al., 2020, A&A, 641, A136

Westergaard N. J., Budtz-Jorgensen C., Chenevez J., Lund N., Brandt S., Oxborrow C. A., 2006, The Astronomer's Telegram, 967, 1

Wijnands R., 2006, The Astronomer's Telegram, 972, 1

Winkler C., et al., 2003, A&A, 411, L1

Winter L. M., Mushotzky R. F., Tueller J., Markwardt C., 2008, ApJ, 674, 686

Winter L. M., Mushotzky R. F., Terashima Y., Ueda Y., 2009, ApJ, 701, 1644

Worpel H., Schwope A. D., Traulsen I., Mukai K., Ok S., 2020, A&A, 639, A17

Xiao G. C., et al., 2019, Journal of High Energy Astrophysics, 24, 30

Xu X., Shao Y., Li X.-D., 2019, MNRAS, 489, 3031

Yatabe F., et al., 2019, The Astronomer's Telegram, 12425, 1

Zhang S., Chen Y. P., Wang J. M., Torres D. F., Li T. P., 2009, A&A, 502, 231

Zhang S., et al., 2015, ApJ, 815, 132

Zolotukhin I. Y., Revnivtsev M. G., 2011, MNRAS, 411, 620

Zolotukhin I. Y., Revnivtsev M. G., 2015, MNRAS, 446, 2418

Zurita Heras J. A., Chaty S., 2008, A&A, 489, 657

Zurita Heras J. A., Chaty S., Tomsick J. A., 2009, A&A, 502, 787

de Rosa A., et al., 2012, MNRAS, 420, 2087

den Hartog P. R., Hermsen W., Kuiper L. M., in't Zand J. J. M., Winkler C., Domingo A., 2004a, The Astronomer's Telegram, 261, 1

den Hartog P. R., Kuiper L. M., Corbet R. H. D., in't Zand J. J. M., Hermsen W., Vink J., Remillard R., van der Klis M., 2004b, The Astronomer's Telegram, 281, 1

den Hartog P. R., Hermsen W., Kuiper L., Vink J., in't Zand J. J. M., Collmar W., 2006, A&A, 451, 587

in 't Zand J., Bazzano A., Cocchi M., Ubertini P., Muller J. M., Torroni V., 1998, IAU Circ., 6846, 2

in't Zand J. J. M., 2005, A&A, 441, L1

APPENDIX A: CATALOG OF SOURCES IN 17–60 KEV BAND

Table A1. The full list of hard X-ray sources detected during the *INTEGRAL* all-sky survey based on 17 years of observations. This catalog is only available in the online version of the paper, at the CDS via anonymous ftp to cdsarc.u-strasbg.fr (130.79.128.5) or via http://cdsarc.u-strasbg.fr/viz-bin/qcat?, and at website http://integral.cosmos.ru.

Id	Name[1]	RA[2] (deg)	Dec[2] (deg)	Flux[3] (17–60 keV)	Type[4]	Notes[5]
N001	SWIFT J0001.6-7701	0.370	-77.020	0.58 ± 0.12	SEYFERT	z=0.058; !B16;
N002	IGR J00040+7020	1.029	70.315	0.86 ± 0.08	SEYFERT	R 1; z=0.096;
N003	**IGR J00115+2645**	2.880	26.760	1.90 ± 0.40	UNIDENT	!B16;
N004	**IGR J00197+6224**	4.930	62.410	0.29 ± 0.06	UNIDENT	!B16;
N005	IGR J00234+6141	5.742	61.686	0.78 ± 0.06	CV	R 2,3;
N006	TYCHO SNR	6.325	64.150	0.76 ± 0.06	SNR	
N007	IGR J00255+6821	6.407	68.362	0.53 ± 0.07	SEYFERT	R 4,1; z=0.012;
N008	V709 Cas	7.201	59.296	5.52 ± 0.06	CV	
N009	IGR J00291+5934	7.263	59.572	1.84 ± 0.06	LMXB	R 5,6;
N010	IGR J00335+6126	8.372	61.469	0.65 ± 0.06	SEYFERT	R 4,7; z=0.105;
N011	SWIFT J0034.5-7904	8.570	-79.089	0.98 ± 0.12	SEYFERT	z=0.074;
N012	1ES 0033+595	8.970	59.822	1.76 ± 0.06	BLAZAR	z=0.086;
N013	IGR J00370+6122	9.275	61.397	1.24 ± 0.06	HMXB	R 8;
N014	NGC 235A	10.757	-23.473	3.86 ± 0.66	SEYFERT	z=0.022; !B16;
N015	MRK 348	12.181	31.951	6.07 ± 0.23	SEYFERT	z=0.015;
N016	RX J0053.8-7226	12.737	-72.226	0.69 ± 0.11	HMXB	in SMC; !B16;
N017	RX J0053.8-7226	13.507	-72.470	0.70 ± 0.10	HMXB	
N018	IGR J00555+4610	13.867	46.195	1.28 ± 0.27	CV	
N019	Gamma Cas	14.178	60.716	5.27 ± 0.07	STAR	Be star;
N020	IGR J00569-7225	14.220	-72.430	1.11 ± 0.10	HMXB	R 9; in SMC;
N021	IGR J00569+6359	14.240	63.990	0.31 ± 0.07	SEYFERT	R 10; z=0.291; !B16;
N022	MRK 0352	14.949	31.935	1.82 ± 0.24	SEYFERT	z=0.015;
N023	IGR J01017+6519	15.440	65.330	0.46 ± 0.07	SEYFERT	R 11; z=0.085; !B16;
N024	IGR J01036-6439	15.920	-64.660	0.91 ± 0.14	BLAZAR	z=0.163; !B16;
N025	IGR J01044-7253	16.110	-72.900	1.16 ± 0.10	HMXB	R 12; in SMC;
N026	**IGR J01062-2436**	16.570	-24.600	2.84 ± 0.61	UNIDENT	!B16;
N027	SMC X-1	19.291	-73.447	26.92 ± 0.11	HMXB	in SMC;
N028	1A 0114+650	19.512	65.288	11.21 ± 0.08	HMXB	
N029	4U 0115+63	19.633	63.740	27.19 ± 0.08	HMXB	
N030	FAIRALL 9	20.950	-58.830	2.70 ± 0.24	SEYFERT	z=0.048;
N031	NGC 0526A	20.998	-35.052	3.22 ± 0.56	SEYFERT	z=0.019;
N032	IGR J01242+3348	21.060	33.800	1.36 ± 0.28	SEYFERT	z=0.020; !B16;
N033	ESO 297- G 018	24.653	-40.010	3.02 ± 0.43	SEYFERT	z=0.025;
N034	4U 0142+61	26.587	61.747	2.93 ± 0.09	MAGNETAR	
N035	RX J0146.9+6121	26.712	61.359	2.02 ± 0.09	HMXB	
N036	IGR J01528-0326	28.221	-3.443	1.53 ± 0.14	SEYFERT	R 13; z=0.017;
N037	IGR J01545+6437	28.625	64.617	0.53 ± 0.10	SEYFERT	R 14,15,16; z=0.035;
N038	IGR J015712-7259	29.318	-72.976	0.49 ± 0.11	HMXB?	R 17; in SMC;
N039	IGR J01583+6713	29.576	67.224	0.44 ± 0.10	HMXB	R 18,19;
N040	NGC 788	30.280	-6.816	4.66 ± 0.13	SEYFERT	z=0.014;
N041	MRK 1018	31.579	-0.300	1.09 ± 0.14	SEYFERT	z=0.043;
N042	SWIFT J0208.4-7428	31.675	-74.470	0.68 ± 0.11	HMXB	in LMC; !B16;
N043	IGR J02086-1742	32.166	-17.649	1.05 ± 0.22	SEYFERT	R 14,20,15; z=0.129;
N044	IGR J02095+5226	32.422	52.446	2.88 ± 0.18	SEYFERT	R 21; z=0.049;
N045	IGR J02145+5142	33.559	51.691	1.06 ± 0.19	BLAZAR	R 22; z=0.049; !B16;
N046	MRK 590	33.635	-0.793	1.09 ± 0.13	SEYFERT	z=0.026;
N047	IGR J02164+5126	34.121	51.439	1.10 ± 0.20	SEYFERT	R 7,23; z=0.422;
N048	QSO B0212+73	34.430	73.844	1.56 ± 0.19	BLAZAR	z=2.367;
N049	MRK 1040	37.053	31.315	3.60 ± 0.29	SEYFERT	z=0.016;
N050	IGR J02343+3229	38.564	32.491	4.33 ± 0.23	SEYFERT	R 24,25; z=0.016;
N051	NGC 0985	38.648	-8.829	1.76 ± 0.14	SEYFERT	z=0.043;
N052	SWIFT J0238.2-5213	39.550	-52.270	1.12 ± 0.25	SEYFERT	z=0.045; !B16;
N053	LSI +61 303	40.100	61.218	1.51 ± 0.13	HMXB	
N054	NGC 1052	40.268	-8.246	1.45 ± 0.15	SEYFERT	z=0.005;
N055	NGC 1068	40.681	-0.003	2.15 ± 0.16	SEYFERT	z=0.004;

<div align="right">Continued on next page</div>

Table A1 – continued from previous page

Id	Name[1]	RA[2] (deg)	Dec[2] (deg)	Flux[3] (17–60 keV)	Type[4]	Notes
N056	SWIFT J0243.6+6124	40.918	61.434	4.56 ± 0.13	HMXB	R 26,27,28; !B16;
N057	4U 0241+61	41.239	62.458	4.99 ± 0.14	SEYFERT	R 29; z=0.045;
N058	SWIFT J0250.2+4650	42.606	46.802	1.36 ± 0.16	SEYFERT	R 30,31; z=0.021; !B16;
N059	IGR J02501+5440	42.677	54.705	1.25 ± 0.15	SEYFERT	R 4,1; z=0.015;
N060	IGR J02524-0829	43.099	-8.489	1.52 ± 0.18	SEYFERT	R 32; z=0.017;
N061	NGC 1142	43.794	-0.193	4.45 ± 0.20	SEYFERT	z=0.029;
N062	XY Ari	44.037	19.468	2.87 ± 0.32	CV	
N063	MCG-02-08-038	45.000	-10.800	1.04 ± 0.23	SEYFERT	z=0.032;
N064	NGC 1194	46.003	-1.106	1.69 ± 0.25	SEYFERT	z=0.013;
N065	SWIFT J0308.5-7251	46.897	-72.834	0.72 ± 0.11	SEYFERT	z=0.028; !B16;
N066	**IGR J03088+3659**	47.220	36.990	0.59 ± 0.13	UNIDENT	!B16;
N067	IGR J03117+5028	47.945	50.466	0.91 ± 0.14	SEYFERT	R 22,33; z=0.062; !B16;
N068	SWIFT J0318.7+6828	49.658	68.465	0.92 ± 0.21	SEYFERT	z=0.090;
N069	Perseus	49.964	41.519	4.81 ± 0.13	CLUSTER	z=0.018; C; E;
N070	1H 0323+342	51.172	34.179	1.52 ± 0.13	SEYFERT	z=0.063;
N071	IGR J03249+4041	51.224	40.698	0.76 ± 0.12	SEYFERT	R 34,35; z=0.048; !B16;
N072	GK Per	52.796	43.886	4.11 ± 0.12	CV	
N073	IGR J03334+3718	53.348	37.300	1.20 ± 0.12	SEYFERT	R 36,24; z=0.055;
N074	NGC 1365	53.424	-36.170	4.21 ± 0.52	SEYFERT	z=0.006;
N075	V0332+53	53.750	53.173	162.68 ± 0.13	HMXB	
N076	4C 32.14	54.115	32.312	2.08 ± 0.13	BLAZAR	z=1.258;
N077	ESO 548-81	55.474	-21.257	3.12 ± 0.50	SEYFERT	z=0.015;
N078	IGR J03526-6830	58.150	-68.510	0.45 ± 0.11	BLAZAR	z=0.087;
N079	SWIFT J0353.7+3711	58.400	37.200	0.60 ± 0.12	SEYFERT	z=0.018;
N080	4U 0352+30	58.846	31.041	40.23 ± 0.14	HMXB	
N081	IGR J03574-6602	59.375	-66.043	0.61 ± 0.12	UNIDENT	R 37,38; !B16;
N082	SWIFT J0359.7+5058	59.931	50.965	0.89 ± 0.12	BLAZAR	z=1.520; !B16;
N083	IGR J04059+5416	61.500	54.280	0.88 ± 0.13	AGN	R 39; !B16;
N084	IGR J04072+0342	61.822	3.700	1.21 ± 0.22	SEYFERT	z=0.089;
N085	**IGR J04085-6546**	62.150	-65.770	0.54 ± 0.11	AGN	R 40; z=0.125; !B16;
N086	SWIFT J0414.8-0754	63.750	-7.920	1.45 ± 0.28	SEYFERT	z=0.038; !B16;
N087	3C 111	64.582	38.021	6.03 ± 0.13	SEYFERT	z=0.049;
N088	NGC 1566	64.960	-54.940	1.78 ± 0.24	SEYFERT	z=0.005; !B16;
N089	IGR J04221+4856	65.530	48.950	0.67 ± 0.12	SEYFERT	R 41,42; z=0.114;
N090	SWIFT J0422.7-5611	65.638	-56.200	1.38 ± 0.21	SEYFERT	z=0.043; !B16;
N091	IGR J04236+0408	65.940	4.136	1.60 ± 0.15	SEYFERT	z=0.046;
N092	1H 0419-577	66.507	-57.201	1.53 ± 0.19	SEYFERT	z=0.104; !B16;
N093	SWIFT J0427.0+0734	66.800	7.250	0.67 ± 0.15	SEYFERT	z=0.097; !B16;
N094	IGR J04288-6702	67.201	-67.040	0.55 ± 0.09	SEYFERT	R 43; z=0.065; !B16; C;
N095	ABELL 3266	67.854	-61.441	0.73 ± 0.12	CLUSTER	z=0.059; !B16;
N096	3C 120	68.304	5.354	5.64 ± 0.12	SEYFERT	z=0.033;
N097	IGR J04379-7240	69.492	-72.669	0.61 ± 0.09	UNIDENT	R 37; !B16;
N098	SWIFT J0440.2-5941	69.996	-59.682	0.77 ± 0.14	SEYFERT	z=0.058; !B16;
N099	RX J0440.9+4431	70.234	44.558	3.48 ± 0.13	HMXB	
N100	PKS 0440-00	70.654	-0.307	0.67 ± 0.10	BLAZAR	z=0.845; !B16;
N101	UGC 3142	70.980	28.987	3.40 ± 0.16	SEYFERT	z=0.022;
N102	SWIFT J0451.5-6949	72.814	-69.799	1.46 ± 0.08	HMXB	in LMC;
N103	MCG -01-13-025	72.921	-3.808	1.08 ± 0.10	SEYFERT	z=0.016;
N104	RX J0452.0+4932	73.034	49.549	2.35 ± 0.13	SEYFERT	z=0.029;
N105	CGCG 420-015	73.382	4.036	1.79 ± 0.09	SEYFERT	z=0.029;
N106	ESO 033-G002	73.963	-75.542	1.23 ± 0.09	SEYFERT	z=0.018;
N107	IGR J04571+4527	74.300	45.458	0.93 ± 0.13	CV	R 15,44;
N108	IGR J05007-7047	75.197	-70.763	1.25 ± 0.08	HMXB	R 45,46; in LMC;
N109	LEDA 075258	75.559	3.525	1.66 ± 0.08	SEYFERT	z=0.016;
N110	V1062 Tau	75.634	24.746	1.31 ± 0.11	CV	
N111	SWIFT J0504.6-7345	76.142	-73.824	0.69 ± 0.09	SEYFERT	z=0.045; !B16;
N112	IGR J05048-7340	76.194	-73.667	0.38 ± 0.09	SEYFERT	z=0.045; !B16;
N113	SWIFT J0505.6-6736	76.352	-67.577	0.82 ± 0.08	AGN	z=0.471; !B16;

Table A1 – continued from previous page

Id	Name[1]	RA[2] (deg)	Dec[2] (deg)	Flux[3] (17–60 keV)	Type[4]	Notes
N114	XSS J05054-2348	76.429	-23.850	3.88 ± 0.29	SEYFERT	z=0.035;
N115	IGR J05081+1722	77.040	17.370	1.39 ± 0.11	SEYFERT	z=0.018;
N116	IGR J05099-6913	77.486	-69.221	0.36 ± 0.08	UNIDENT	R 43; !B16;
N117	IRAS 05078+1626	77.684	16.497	4.89 ± 0.11	SEYFERT	z=0.018;
N118	4U 0513-40	78.523	-40.064	3.42 ± 0.33	LMXB	
N119	SWIFT J0515.3+1854	78.840	18.900	1.40 ± 0.10	SEYFERT	R 47; z=0.023;
N120	ARK 120	79.040	-0.145	4.09 ± 0.08	SEYFERT	z=0.032;
N121	IGR J05162-1034	79.070	-10.570	0.88 ± 0.14	SEYFERT	z=0.029; !B16;
N122	ESO 362-18	79.900	-32.657	2.84 ± 0.23	SEYFERT	z=0.013;
N123	PICTOR A	79.937	-45.770	2.51 ± 0.47	SEYFERT	z=0.035;
N124	LMC X-2	80.040	-71.951	0.97 ± 0.08	LMXB	in LMC;
N125	RX J0520.5-6932	80.123	-69.532	0.57 ± 0.08	HMXB	R 48; in LMC; !B16;
N126	PKS 0521-36	80.683	-36.463	1.65 ± 0.25	BLAZAR	z=0.055;
N127	RX J0525.3+2413	81.392	24.218	0.80 ± 0.09	CV	
N128	TV COL	82.355	-32.813	4.65 ± 0.22	CV	
N129	IGR J05305-6559	82.548	-65.857	0.49 ± 0.08	HMXB	R 43; in LMC;
N130	SWIFT J053041.9-665426	82.660	-66.890	0.45 ± 0.08	HMXB	R 49; in LMC; !B16;
N131	PKS 0528+134	82.739	13.563	0.59 ± 0.10	BLAZAR	z=2.060;
N132	IGR J05305-6559	82.805	-66.118	2.17 ± 0.08	HMXB	R 43; in LMC; C;
N133	LMC X-4	83.192	-66.368	30.56 ± 0.08	HMXB	in LMC;
N134	IGR J05329-7051	83.242	-70.854	0.38 ± 0.08	BLAZAR?	R 37; z=1.238; !B16;
N135	Crab	83.632	22.018	1345.73 ± 0.09	SNR / PULSAR	
N136	IGR J05342-6016	83.657	-60.269	1.09 ± 0.11	SEYFERT	z=0.057; !B16;
N137	TW Pic	83.682	-57.989	1.44 ± 0.14	CV	
N138	IGR J05373-8424	84.342	-84.408	0.99 ± 0.19	UNIDENT	R 37; !B16;
N139	PSR J0537-6910	84.444	-69.171	0.65 ± 0.08	SNR / PULSAR	in LMC; !B16; C;
N140	LMC X-3	84.704	-64.117	0.79 ± 0.09	HMXB	in LMC; !B16;
N141	A 0535+262	84.733	26.343	163.32 ± 0.09	HMXB	T;
N142	LMC X-1	84.911	-69.746	2.24 ± 0.08	HMXB	in LMC;
N143	PKS 0537-286	84.968	-28.676	1.31 ± 0.20	BLAZAR	z=3.104;
N144	PSR B0540-69	85.001	-69.338	2.69 ± 0.08	SNR / PULSAR	in LMC;
N145	IGR J05414-6858	85.361	-69.024	0.83 ± 0.08	HMXB	in LMC; C;
N146	XMMU J054134.7-682550	85.437	-68.430	0.53 ± 0.08	HMXB	in LMC; !B16;
N147	BY Cam	85.729	60.847	2.28 ± 0.30	CV	
N148	IGR J05470+5034	86.750	50.580	1.49 ± 0.21	SEYFERT	R 31; z=0.036;
N149	NGC 2110	88.047	-7.462	13.41 ± 0.13	SEYFERT	z=0.008;
N150	MCG+08-11-011	88.734	46.437	10.32 ± 0.22	SEYFERT	z=0.021;
N151	V405 Aur	89.507	53.892	2.84 ± 0.26	CV	
N152	SWIFT J0600.7+0008	90.190	0.100	0.67 ± 0.12	SEYFERT	z=0.114; !B16;
N153	IRAS 05589+2828	90.556	28.477	3.77 ± 0.11	SEYFERT	z=0.033;
N154	ESO 005- G 004	91.415	-86.632	1.70 ± 0.24	SEYFERT	z=0.006;
N155	IGR J06058-2755	91.471	-27.934	1.19 ± 0.24	SEYFERT	R 15; z=0.089;
N156	IGR J06075-6148	91.874	-61.808	0.59 ± 0.11	AGN	z=0.004; !B16;
N157	MRK 3	93.901	71.040	7.90 ± 0.20	SEYFERT	z=0.014;
N158	4U 0614+091	94.283	9.135	23.69 ± 0.17	LMXB	
N159	IGR J06233-6436	95.776	-64.598	0.61 ± 0.09	BLAZAR	z=0.129; !B16;
N160	ESO 426-G 002	95.960	-32.206	1.45 ± 0.32	SEYFERT	z=0.022;
N161	IGR J06239-6052	95.960	-60.963	1.84 ± 0.12	SEYFERT	R 50; z=0.040;
N162	IGR J06253+7334	96.303	73.551	1.43 ± 0.18	CV	
N163	SWIFT J0634.7-7445	98.637	-74.758	0.63 ± 0.10	SEYFERT	z=0.112; !B16;
N164	IGR J06354-7516	98.858	-75.282	0.77 ± 0.10	BLAZAR	z=0.651;
N165	IGR J06380-7536	99.430	-75.646	0.63 ± 0.10	SEYFERT	z=0.089; !B16;
N166	IGR J06402-2552	100.052	-25.883	2.17 ± 0.31	SEYFERT	z=0.025;
N167	IGR J06415+3251	100.366	32.878	2.31 ± 0.28	SEYFERT	R 51; z=0.047;
N168	IGR J06503-7742	102.477	-77.704	0.76 ± 0.12	AGN	z=0.037; !B16;
N169	MRK 6	103.054	74.425	3.22 ± 0.15	SEYFERT	z=0.019;
N170	FAIRALL 265	104.124	-65.560	0.77 ± 0.11	SEYFERT	z=0.030; !B16;
N171	IGR J06571+7802	104.277	78.044	0.75 ± 0.15	UNIDENT	R 37; !B16;

Table A1 – continued from previous page

Id	Name[1]	RA[2] (deg)	Dec[2] (deg)	Flux[3] (17–60 keV)	Type[4]	Notes
N172	MXB 0656-072	104.567	-7.215	4.22 ± 0.16	HMXB	
N173	IGR J07072-1227	106.810	-12.460	0.78 ± 0.14	UNIDENT	R 52;
N174	SWIFT J0710.5+5908	107.613	59.141	1.85 ± 0.29	BLAZAR	z=0.125; !B16;
N175	IGR J07141+0146	108.540	1.770	1.28 ± 0.24	UNIDENT	R 53; !B16;
N176	S5 0716+714	110.510	71.320	0.65 ± 0.12	BLAZAR	z=0.300; !B16;
N177	PKS 0723-008	111.480	-0.926	1.12 ± 0.22	BLAZAR	z=0.128;
N178	IGR J07264-3553	111.611	-35.883	1.18 ± 0.28	SEYFERT	z=0.029; !B16;
N179	SWIFT J0728.8-2605	112.201	-26.091	1.84 ± 0.17	HMXB	
N180	IGR J07296-5854	112.413	-58.905	0.96 ± 0.22	UNIDENT	R 37; !B16;
N181	SWIFT J0732.5-1331	113.126	-13.491	2.15 ± 0.13	CV	
N182	**IGR J07328-4640**	113.214	-46.682	0.72 ± 0.16	BLAZAR?	PKS 0731-465; !B16;
N183	IGR J07396-3143	114.902	-31.742	1.73 ± 0.21	SEYFERT	R 22; z=0.026; !B16;
N184	MRK 79	115.637	49.810	4.26 ± 0.68	SEYFERT	z=0.022;
N185	IGR J07433-2544	115.840	-25.762	1.26 ± 0.15	SEYFERT	R 22; z=0.023; !B16;
N186	SWIFT J0747.9-7327	116.984	-73.455	0.87 ± 0.13	SEYFERT	z=0.036; !B16;
N187	EXO 0748-676	117.140	-67.757	5.66 ± 0.15	LMXB	
N188	IGR J07563-4137	119.074	-41.637	0.90 ± 0.11	SEYFERT	R 54,45; z=0.021;
N189	IGR J07563+5919	119.091	59.321	0.83 ± 0.21	UNIDENT	R 37; !B16;
N190	IGR J07597-3842	119.926	-38.726	2.91 ± 0.12	SEYFERT	R 55,46; z=0.040;
N191	IGR J08004-4309	120.115	-43.155	0.52 ± 0.10	CV	R 22,56;
N192	ESO 209-G012	120.500	-49.752	1.69 ± 0.11	SEYFERT	z=0.041;
N193	MRK 1210	121.041	5.109	4.09 ± 0.54	SEYFERT	z=0.014;
N194	PG 0804+761	122.814	76.047	0.92 ± 0.09	SEYFERT	z=0.100;
N195	IGR J08190-3835	124.759	-38.583	0.44 ± 0.10	SEYFERT	R 57; z=0.009;
N196	RX J0818.9-2252	124.780	-22.890	0.75 ± 0.16	SEYFERT	z=0.035; !B16;
N197	IGR J08215-1320	125.390	-13.340	0.99 ± 0.14	SEYFERT	R 11; z=0.015; !B16;
N198	SWIFT J0823.4-0457	125.752	-4.913	1.80 ± 0.23	SEYFERT	z=0.022; !B16;
N199	SWIFT J0826.2-7033	126.475	-70.577	1.25 ± 0.18	CV	!B16;
N200	IGR J08297-4250	127.450	-42.840	0.54 ± 0.08	AGN	R 39; !B16;
N201	IGR J08321-1808	128.030	-18.150	1.05 ± 0.15	SEYFERT	R 53,11; z=0.135; !B16;
N202	Vela pulsar	128.835	-45.179	9.07 ± 0.08	SNR / PULSAR	
N203	SWIFT J0835.5-0902	128.882	-9.070	1.31 ± 0.17	AGN?	!B16;
N204	NGC 2617	128.912	-4.088	4.05 ± 0.24	SEYFERT	z=0.014; !B16;
N205	GS 0834-43	128.979	-43.185	0.93 ± 0.08	HMXB	!B16;
N206	4U 0836-429	129.349	-42.897	15.39 ± 0.08	LMXB	
N207	FAIRALL 1146	129.634	-35.986	1.79 ± 0.11	SEYFERT	z=0.032;
N208	IGR J08390-4833	129.681	-48.521	0.76 ± 0.08	CV	R 58,59,60;
N209	3C 206	129.961	-12.243	1.77 ± 0.15	SEYFERT	z=0.198; !B16;
N210	S5 0836+71	130.353	70.905	4.47 ± 0.08	BLAZAR	z=2.170;
N211	IGR J08453-3529	131.341	-35.488	0.66 ± 0.12	SEYFERT	R 15; z=0.137;
N212	IGR J08503+6630	132.580	66.500	0.51 ± 0.08	UNIDENT	R 37; !B16;
N213	NGC 2655	133.860	78.220	0.55 ± 0.09	AGN	z=0.005; !B16;
N214	IGR J08557+6420	133.887	64.361	0.75 ± 0.09	SEYFERT	R 15; z=0.036;
N215	Vela X-1	135.531	-40.556	278.79 ± 0.09	HMXB	
N216	IGR J09026-4812	135.650	-48.229	1.61 ± 0.08	SEYFERT	R 61; z=0.039;
N217	IGR J09025-6814	135.664	-68.227	1.34 ± 0.17	AGN	R 7; z=0.013;
N218	1RXS J090431.1-382920	136.130	-38.489	0.55 ± 0.10	SEYFERT	R 47; z=0.016;
N219	**IGR J09082-1336**	137.070	-13.610	0.89 ± 0.18	UNIDENT	!B16;
N220	ABELL 754	137.230	-9.700	0.83 ± 0.19	CLUSTER	z=0.054; !B16;
N221	SWIFT J0911.9-6452	138.010	-64.868	5.07 ± 0.13	LMXB	R 62; !B16;
N222	IRAS 09149-6206	139.036	-62.333	1.80 ± 0.12	SEYFERT	z=0.057;
N223	IGR J09189-4418	139.731	-44.312	0.36 ± 0.09	SEYFERT?	R 63,16;
N224	4U 0919-54	140.098	-55.206	5.29 ± 0.09	LMXB	
N225	SWIFT J0920.8-0805	140.190	-8.050	3.09 ± 0.22	SEYFERT	z=0.020;
N226	PKS 0921-213	140.930	-21.630	1.30 ± 0.28	BLAZAR	z=0.052; !B16;
N227	MRK 110	141.276	52.296	4.79 ± 0.22	SEYFERT	z=0.036;
N228	IGR J09253+6929	141.439	69.470	0.88 ± 0.07	SEYFERT	R 64,65,37; z=0.040;
N229	IGR J09278-3935	141.970	-39.590	0.53 ± 0.11	UNIDENT	R 53; !B16;

Table A1 – continued from previous page

Id	Name[1]	RA[2] (deg)	Dec[2] (deg)	Flux[3] (17–60 keV)	Type[4]	Notes
N230	SWIFT J0929.7+6232	142.390	62.537	0.71 ± 0.09	SEYFERT	R 47; z=0.026;
N231	IGR J09331-4725	143.280	-47.430	0.50 ± 0.09	UNIDENT	R 53; !B16;
N232	SWIFT J0935.9+6120	143.965	61.353	0.51 ± 0.09	SEYFERT	z=0.039; !B16;
N233	NGC 2992	146.434	-14.329	3.83 ± 0.23	SEYFERT	R 66; z=0.008;
N234	MCG-05-23-16	146.922	-30.947	11.87 ± 0.29	SEYFERT	z=0.008;
N235	SWIFT J0950.5+7318	147.496	73.253	0.57 ± 0.07	SEYFERT	R 37; z=0.058;
N236	IGR J09522-6231	148.069	-62.536	0.76 ± 0.09	SEYFERT	R 58,57; z=0.252;
N237	M81	148.888	69.065	1.32 ± 0.07	SEYFERT	
N238	M82 X-1	148.958	69.679	0.47 ± 0.07	ULX	!B16;
N239	HolX X-1	149.472	69.063	0.27 ± 0.07	ULX	
N240	SWIFT J0958.0-4208	149.487	-42.133	1.55 ± 0.14	CV?	R 67;
N241	SWIFT J0958.2-5732	149.650	-57.450	0.42 ± 0.08	UNIDENT	R 38; !B16;
N242	NGC 3081	149.870	-22.819	4.72 ± 0.29	SEYFERT	z=0.008;
N243	NGC 3079	150.491	55.680	2.13 ± 0.16	SEYFERT	z=0.004;
N244	GRO J1008-57	152.419	-58.282	7.19 ± 0.08	HMXB	
N245	ESO 263-13	152.463	-42.799	1.39 ± 0.16	SEYFERT	z=0.033;
N246	IGR J10100-5655	152.523	-56.916	0.70 ± 0.08	HMXB	R 68,46,69;
N247	IGR J10109-5746	152.774	-57.797	1.53 ± 0.08	CV	R 70,71;
N248	NGC 3227	155.873	19.870	8.50 ± 0.44	SEYFERT	z=0.004;
N249	IGR J10252+6716	156.310	67.310	0.48 ± 0.07	SEYFERT	R 37; z=0.039; !B16;
N250	**IGR J10257+4532**	156.430	45.550	1.14 ± 0.24	UNIDENT	!B16;
N251	ESO 317-41	157.850	-42.090	0.90 ± 0.20	AGN	z=0.020; !B16;
N252	NGC 3281	157.961	-34.860	4.84 ± 0.27	SEYFERT	z=0.011;
N253	SWIFT J1033.6+7303	158.378	73.087	0.45 ± 0.07	SEYFERT?	R 37,33; z=0.022; !B16;
N254	4U 1036-56	159.454	-56.745	1.18 ± 0.07	HMXB	
N255	IGR J10380+8435	159.513	84.587	0.86 ± 0.20	UNIDENT	R 37; !B16;
N256	IGR J10386-4947	159.672	-49.790	1.33 ± 0.10	SEYFERT	R 72; z=0.060;
N257	IGR J10404-4625	160.134	-46.386	1.32 ± 0.14	SEYFERT	R 54,73; z=0.024;
N258	SWIFT J1044.1+7024	161.061	70.355	0.69 ± 0.07	SEYFERT	R 22; z=0.033; !B16;
N259	IGR J10447-6027	161.156	-60.448	0.77 ± 0.07	SEYFERT?	R 74,75,76,77; z=0.047;
N260	S5 1039+81	161.220	80.890	0.73 ± 0.12	BLAZAR	R 37; z=1.260; !B16;
N261	ETA CAR	161.221	-59.707	0.72 ± 0.07	STAR	
N262	**IGR J10595-5125**	164.880	-51.420	0.45 ± 0.09	SEYFERT	z=0.019; ESO 215-14; !B16;
N263	IGR J11014-6103	165.440	-61.000	0.41 ± 0.07	SNR / PULSAR	R 52;
N264	4C 72.16	165.453	72.427	0.44 ± 0.08	BLAZAR	R 37; z=1.460; !B16;
N265	IGR J11030+7027	165.740	70.497	0.38 ± 0.08	UNIDENT	R 37; !B16;
N266	MRK 421	166.116	38.210	18.28 ± 0.14	BLAZAR	z=0.031;
N267	**IGR J11054-1120**	166.350	-11.350	2.89 ± 0.64	UNIDENT	!B16;
N268	SWIFT J1105.7+5854	166.423	58.914	1.04 ± 0.15	SEYFERT?	R 37; !B16;
N269	NGC 3516	166.718	72.559	2.61 ± 0.08	SEYFERT	z=0.009;
N270	IGR J11079+7106	166.992	71.109	0.48 ± 0.08	SEYFERT	R 78; z=0.060; !B16;
N271	**IGR J11131-5853**	168.290	-58.890	0.34 ± 0.07	UNIDENT	!B16;
N272	**IGR J11176+1707**	169.410	17.120	3.03 ± 0.63	UNIDENT	!B16;
N273	IGR J11187-5438	169.592	-54.662	0.79 ± 0.08	LMXB?	R 79,69;
N274	1A 1118-61	170.238	-61.917	2.82 ± 0.07	HMXB	
N275	Cen X-3	170.313	-60.624	63.85 ± 0.07	HMXB	
N276	IGR J11215-5952	170.440	-59.870	0.67 ± 0.07	HMXB	R 80,81,82;
N277	PSR J1124-5916	171.130	-59.240	0.35 ± 0.07	SNR / PULSAR	!B16;
N278	IGR J11275-5319	171.890	-53.330	0.79 ± 0.09	UNIDENT	!B16;
N279	IGR J11299-6557	172.490	-65.960	0.43 ± 0.09	AGN?	R 11;
N280	IGR J11305-6256	172.779	-62.948	1.56 ± 0.08	HMXB	R 83,3,73;
N281	IGR J11361-6003	174.089	-60.064	0.72 ± 0.08	SEYFERT	R 1; z=0.014;
N282	RX J1136.5+6737	174.125	67.618	0.66 ± 0.10	BLAZAR	R 37; z=0.134; !B16;
N283	NGC 3783	174.747	-37.759	9.13 ± 0.49	SEYFERT	z=0.010;
N284	GT Mus	174.875	-65.398	0.42 ± 0.08	STAR	
N285	DO Dra	175.910	71.689	0.61 ± 0.10	CV	!B16;
N286	IGR J11435-6109	175.996	-61.123	4.08 ± 0.08	HMXB	R 84,7,85,69;
N287	SWIFT J1144.1+3652	176.119	36.904	0.72 ± 0.12	SEYFERT	R 22; z=0.038; !B16;

Continued on next page

Table A1 – continued from previous page

Id	Name[1]	RA[2] (deg)	Dec[2] (deg)	Flux[3] (17–60 keV)	Type[4]	Notes
N288	MCG+13-09-002	176.318	79.681	1.34 ± 0.13	SEYFERT	R 37; z=0.015;
N289	HE 1143-1810	176.420	-18.460	3.38 ± 0.47	SEYFERT	z=0.033;
N290	PKS 1143-696	176.509	-69.943	0.90 ± 0.11	BLAZAR	z=0.243;
N291	1E 1145.1-6141	176.863	-61.971	23.90 ± 0.08	HMXB	
N292	RX J1147.9+0902	176.979	9.041	0.57 ± 0.10	SEYFERT	R 37; z=0.069; !B16;
N293	4U 1145-619	177.000	-62.207	2.60 ± 0.08	HMXB	
N294	IGR J11485+2936	177.130	29.610	0.78 ± 0.18	SEYFERT	R 37; z=0.023; !B16;
N295	**IGR J11523+0713**	178.090	7.230	0.42 ± 0.09	UNIDENT	!B16;
N296	7C 1150+3324	178.216	33.122	0.64 ± 0.14	BLAZAR	R 37; z=1.394; !B16;
N297	SWIFT J1200.8+0650	180.242	6.809	1.16 ± 0.08	SEYFERT	R 37; z=0.036;
N298	MRK 1310	180.350	-3.650	0.51 ± 0.12	SEYFERT	R 37; z=0.020; !B16;
N299	IGR J12024-1127	180.622	-11.460	1.09 ± 0.24	UNIDENT	R 37; !B16;
N300	IGR J12026-5349	180.680	-53.835	3.13 ± 0.10	SEYFERT	R 70,45; z=0.028;
N301	NGC 4051	180.778	44.520	2.37 ± 0.13	SEYFERT	z=0.002;
N302	NGC 4074	181.110	20.291	0.94 ± 0.13	SEYFERT	z=0.023;
N303	MCG+05-29-005	181.184	31.144	0.69 ± 0.14	SEYFERT	z=0.025; !B16;
N304	NGC 4102	181.575	52.714	2.05 ± 0.26	SEYFERT	R 86; z=0.003; !B16;
N305	B2 1204+34	181.887	33.878	0.95 ± 0.12	SEYFERT	R 37; z=0.079; !B16;
N306	IGR J12086-6327	182.160	-63.450	0.33 ± 0.08	UNIDENT	R 53; !B16;
N307	MRK 198	182.316	47.087	1.24 ± 0.15	SEYFERT	z=0.024;
N308	NGC 4138	182.384	43.687	1.65 ± 0.12	SEYFERT	z=0.003;
N309	IGR J12095-0420	182.394	-4.344	0.47 ± 0.11	UNIDENT	R 37; !B16;
N310	NGC 4151	182.635	39.406	35.59 ± 0.11	SEYFERT	z=0.003;
N311	IGR J12107+3822	182.680	38.336	1.17 ± 0.11	SEYFERT	R 87,15; z=0.023;
N312	IGR J12123-5802	183.108	-58.006	0.63 ± 0.09	CV	R 15;
N313	IGR J12131+0700	183.253	7.040	0.87 ± 0.06	SEYFERT	R 1,37; z=0.210;
N314	4U 1210-64	183.255	-64.880	0.57 ± 0.09	HMXB	R 88;
N315	IGR J12134-6015	183.368	-60.252	0.54 ± 0.08	AGN?	R 89;
N316	Was 49	183.574	29.529	0.74 ± 0.14	SEYFERT	z=0.064; !B16;
N317	IGR J12171+7047	184.288	70.797	0.62 ± 0.13	SEYFERT	R 37,78; z=0.007; !B16;
N318	NGC 4235	184.293	7.198	2.84 ± 0.06	SEYFERT	z=0.007;
N319	NGC 4253	184.601	29.820	1.74 ± 0.14	SEYFERT	z=0.013;
N320	NGC 4258	184.721	47.290	1.17 ± 0.15	SEYFERT	R 37; z=0.002;
N321	PKS 1217+02	185.050	2.062	0.59 ± 0.07	SEYFERT	z=0.240;
N322	IGR J12204+0452	185.120	4.868	0.56 ± 0.06	UNIDENT	R 37; !B16;
N323	IGR J12208-0711	185.212	-7.192	0.80 ± 0.12	UNIDENT	R 37; !B16;
N324	3A 1218+303	185.331	30.169	0.85 ± 0.13	BLAZAR	R 22; z=0.184;
N325	MRK 205	185.433	75.311	1.12 ± 0.13	SEYFERT	z=0.071; !B16;
N326	PKS 1219+04	185.598	4.220	1.10 ± 0.06	BLAZAR	z=0.966;
N327	IGR J12224+0306	185.606	3.110	0.44 ± 0.06	BLAZAR?	R 37; !B16;
N328	MRK 50	185.837	2.679	1.24 ± 0.06	SEYFERT	z=0.024;
N329	4C 21.35	186.216	21.394	1.01 ± 0.11	BLAZAR	z=0.434;
N330	NGC 4388	186.447	12.664	12.32 ± 0.07	SEYFERT	R 90; z=0.009;
N331	NGC 4395	186.463	33.556	1.50 ± 0.12	SEYFERT	z=0.001;
N332	GX 301-2	186.654	-62.773	214.10 ± 0.08	HMXB	
N333	XSS J12270-4859	187.000	-48.893	1.60 ± 0.15	LMXB	
N334	3C273	187.277	2.054	16.64 ± 0.06	BLAZAR	z=0.158;
N335	IGR J12304+0946	187.620	9.776	0.27 ± 0.06	UNIDENT	R 37; !B16;
N336	1ES 1229+71.0	187.902	70.737	0.71 ± 0.15	SEYFERT	z=0.208; !B16;
N337	RT Cru	188.721	-64.566	5.16 ± 0.09	CV	
N338	NGC 4507	188.903	-39.905	11.04 ± 0.18	SEYFERT	z=0.012;
N339	IGR J12375+2156	189.392	21.944	0.55 ± 0.11	UNIDENT	R 37; !B16;
N340	NGC 4579	189.432	11.818	0.65 ± 0.06	SEYFERT	R 37; z=0.006; !B16;
N341	SWIFT J1238.6+0929	189.641	9.491	0.56 ± 0.06	SEYFERT	R 47; z=0.083;
N342	ESO 506-G027	189.728	-27.315	4.36 ± 0.38	SEYFERT	z=0.025;
N343	XSS J12389-1614	189.775	-16.182	2.29 ± 0.22	SEYFERT	R 70,45; z=0.037;
N344	NGC 4593	189.910	-5.347	4.71 ± 0.10	SEYFERT	z=0.008;
N345	SWIFT J1240.9+2735	190.229	27.531	0.70 ± 0.13	SEYFERT	R 22,91; z=0.057; !B16;

Table A1 – continued from previous page

Id	Name[1]	RA[2] (deg)	Dec[2] (deg)	Flux[3] (17–60 keV)	Type[4]	Notes
N346	IGR J12412+3007	190.334	30.122	0.83 ± 0.12	AGN?	R 37,92; !B16;
N347	IGR J12415-5750	190.376	-57.827	2.47 ± 0.09	SEYFERT	R 7; z=0.024;
N348	IGR J12418+7805	190.650	78.122	0.76 ± 0.16	SEYFERT	R 37; z=0.022; !B16;
N349	IGR J12480-5829	192.048	-58.448	0.71 ± 0.09	SEYFERT	R 14,15; z=0.028;
N350	IGR J12489-5930	192.240	-59.500	0.53 ± 0.09	UNIDENT	R 53; !B16;
N351	4U 1246-588	192.411	-59.090	4.69 ± 0.09	LMXB	
N352	NGC 4736	192.721	41.120	0.68 ± 0.13	SEYFERT	R 37; z=0.001; !B16;
N353	NGC 4748	193.087	-13.432	0.99 ± 0.18	SEYFERT	z=0.014;
N354	IGR J12529-6351	193.240	-63.850	0.38 ± 0.08	UNIDENT	R 53,93; !B16;
N355	ESO 323-G032	193.315	-41.594	0.76 ± 0.14	SEYFERT	R 22; z=0.016;
N356	PKS 1252+11	193.659	11.685	0.47 ± 0.07	BLAZAR	R 37; z=0.872; !B16;
N357	3C 279	194.047	-5.795	1.52 ± 0.11	BLAZAR	z=0.536;
N358	4U 1254-69	194.419	-69.289	2.41 ± 0.10	LMXB	
N359	Coma	194.880	27.951	1.50 ± 0.12	CLUSTER	z=0.023; E;
N360	SWIFT J1300.1+1635	195.022	16.537	0.37 ± 0.09	SEYFERT	z=0.080; !B16;
N361	4U 1258-61	195.322	-61.602	19.00 ± 0.08	HMXB	
N362	1RXP J130159.6-635806	195.495	-63.969	2.09 ± 0.08	HMXB	R 94,69;
N363	PSR B1259-63	195.699	-63.836	1.18 ± 0.08	HMXB	R 95;
N364	MRK 783	195.700	16.376	1.20 ± 0.09	SEYFERT	z=0.067;
N365	IGR J13038+5348	195.997	53.792	0.92 ± 0.16	SEYFERT	R 36,96; z=0.030;
N366	NGC 4941	196.015	-5.545	0.73 ± 0.12	SEYFERT	z=0.004;
N367	NGC 4939	196.059	-10.328	1.07 ± 0.16	SEYFERT	z=0.010;
N368	IGR J13045-5630	196.110	-56.600	0.74 ± 0.09	UNIDENT	
N369	NGC 4945	196.363	-49.466	15.47 ± 0.12	SEYFERT	z=0.002;
N370	ESO 323-G077	196.620	-40.422	2.56 ± 0.12	SEYFERT	z=0.015;
N371	IGR J13091+1137	197.283	11.629	2.72 ± 0.09	SEYFERT	R 70,45; z=0.025;
N372	IGR J13107-5626	197.655	-56.449	0.70 ± 0.09	AGN?	R 97;
N373	IGR J13107-5551	197.697	-55.876	1.55 ± 0.09	SEYFERT	R 70,1; z=0.104;
N374	PG 1310-108	198.274	-11.128	0.83 ± 0.19	SEYFERT	z=0.034;
N375	NGC 5033	198.364	36.594	0.80 ± 0.16	SEYFERT	z=0.003; !B16;
N376	IGR J13149+4422	198.787	44.419	1.25 ± 0.16	SEYFERT	R 98,25; z=0.036;
N377	IGR J13168-7157	199.196	-71.945	0.75 ± 0.12	SEYFERT	R 99,15; z=0.070;
N378	RX J1317.0+3735	199.262	37.592	0.83 ± 0.17	SEYFERT	z=0.195; !B16;
N379	IGR J13186-6257	199.636	-62.954	0.95 ± 0.08	HMXB	R 100,101,76;
N380	SWIFT J1321.2+0859	200.241	8.950	0.75 ± 0.10	AGN	R 22,102; z=0.033;
N381	MCG-03-34-064	200.611	-16.733	1.62 ± 0.30	SEYFERT	z=0.017;
N382	SAX J1324.5-6313	201.161	-63.228	0.43 ± 0.08	LMXB	R 103;
N383	Cen A	201.362	-43.019	57.38 ± 0.11	SEYFERT	z=0.002;
N384	4U 1323-62	201.653	-62.135	14.15 ± 0.08	LMXB	
N385	ABELL 1736	202.072	-27.293	1.22 ± 0.21	CLUSTER	z=0.046; !B16;
N386	IGR J13290-6323	202.268	-63.392	0.40 ± 0.08	UNIDENT	
N387	**IGR J13292-4332**	202.320	-43.550	0.54 ± 0.11	UNIDENT	!B16;
N388	ESO 509- G038	202.722	-25.412	1.37 ± 0.24	SEYFERT	z=0.026; !B16;
N389	IGR J13310-1355	202.756	-13.931	1.43 ± 0.31	UNIDENT	R 37; !B16;
N390	ESO 383-G018	203.362	-34.028	1.41 ± 0.14	SEYFERT	z=0.013;
N391	MCG-6-30-15	203.982	-34.297	2.37 ± 0.14	SEYFERT	z=0.008;
N392	NGC 5252	204.570	4.548	6.10 ± 0.14	SEYFERT	z=0.023;
N393	IGR J13402-6428	205.080	-64.480	0.35 ± 0.08	UNIDENT	R 52;
N394	MRK 268	205.297	30.378	1.63 ± 0.16	SEYFERT	z=0.040;
N395	NGC 5273	205.555	35.712	1.45 ± 0.20	SEYFERT	R 22; z=0.003; !B16;
N396	IGR J13466+1921	206.676	19.385	0.66 ± 0.16	SEYFERT	z=0.084;
N397	4U 1344-60	206.897	-60.615	6.68 ± 0.08	SEYFERT	z=0.013;
N398	IGR J13486+1554	207.168	15.901	0.72 ± 0.15	UNIDENT	R 37; !B16;
N399	IC 4329A	207.332	-30.312	15.34 ± 0.17	SEYFERT	z=0.016;
N400	TOL 1351-375	208.561	-37.775	0.94 ± 0.11	SEYFERT	z=0.052;
N401	IGR J13545-5958	208.626	-59.963	0.41 ± 0.08	UNIDENT	R 53; !B16;
N402	Ginga 1354-64	209.541	-64.735	3.16 ± 0.08	LMXB	!B16;
N403	IGR J14003-6326	210.142	-63.428	1.20 ± 0.08	SNR / PULSAR	R 104,105;

Table A1 – continued from previous page

Id	Name[1]	RA[2] (deg)	Dec[2] (deg)	Flux[3] (17–60 keV)	Type[4]	Notes
N404	IGR J14044-6146	211.120	-61.780	0.61 ± 0.08	UNIDENT	R 53,52,106;
N405	IGR J14080-3023	212.010	-30.391	1.06 ± 0.16	SEYFERT	R 22; z=0.025;
N406	V834 Cen	212.262	-45.269	0.59 ± 0.11	CV	
N407	IGR J14091-6108	212.280	-61.140	0.49 ± 0.08	CV	R 107; !B16;
N408	SWIFT J1410.9-4229	212.640	-42.459	0.43 ± 0.10	SEYFERT	R 22; z=0.035;
N409	Circinus galaxy	213.291	-65.341	17.93 ± 0.09	SEYFERT	z=0.001;
N410	NGC 5506	213.305	-3.210	12.74 ± 0.21	SEYFERT	z=0.006;
N411	PKS 1413-36	214.180	-36.650	0.60 ± 0.11	AGN	z=0.075; !B16;
N412	IGR J14175-4641	214.266	-46.681	1.34 ± 0.11	SEYFERT	R 70,46; z=0.076;
N413	NGC 5548	214.507	25.139	6.01 ± 0.18	SEYFERT	z=0.017;
N414	AX J1418.7-6058	214.701	-60.915	0.42 ± 0.08	SNR / PULSAR	R 22;
N415	ESO 511-G030	214.834	-26.648	2.15 ± 0.20	SEYFERT	z=0.023;
N416	4U 1416-62	215.285	-62.680	2.04 ± 0.08	HMXB	
N417	3A 1422+481	215.388	47.741	0.95 ± 0.14	SEYFERT	z=0.072;
N418	IGR J14257-6117	216.430	-61.290	0.61 ± 0.08	CV	R 67,108;
N419	H 1426+428	217.072	42.664	1.12 ± 0.19	BLAZAR	z=0.129;
N420	MRK 1383	217.278	1.280	0.90 ± 0.19	SEYFERT	z=0.087; !B16;
N421	IGR J14298-6715	217.440	-67.239	0.98 ± 0.09	LMXB	R 104,1;
N422	**IGR J14300+0118**	217.510	1.310	1.00 ± 0.19	UNIDENT	!B16; C;
N423	NGC 5643	218.172	-44.209	1.18 ± 0.10	SEYFERT	z=0.004;
N424	IGR J14331-6112	218.270	-61.260	0.54 ± 0.08	HMXB	R 104,1,69;
N425	NGC 5674	218.468	5.458	1.17 ± 0.18	SEYFERT	z=0.025;
N426	MRK 817	219.092	58.794	1.41 ± 0.15	SEYFERT	z=0.031; !B16;
N427	HE 1434-1600	219.155	-16.192	2.31 ± 0.26	SEYFERT	z=0.145;
N428	MRK 477	220.156	53.510	1.03 ± 0.14	SEYFERT	z=0.038; !B16;
N429	IGR J14417-5533	220.430	-55.550	0.72 ± 0.08	UNIDENT	R 53; !B16;
N430	NGC 5728	220.588	-17.246	5.07 ± 0.26	SEYFERT	z=0.009;
N431	IGR J14471-6414	221.582	-64.276	0.77 ± 0.09	SEYFERT	R 104,1; z=0.053;
N432	IGR J14471-6319	221.789	-63.288	0.55 ± 0.08	SEYFERT	R 70,46; z=0.038;
N433	IGR J14488-4009	222.199	-40.148	1.01 ± 0.10	SEYFERT	R 67,109; z=0.123;
N434	IGR J14493-5534	222.313	-55.596	1.56 ± 0.08	AGN	R 58; z=0.002;
N435	IGR J14488-5942	222.320	-59.760	0.87 ± 0.08	HMXB	R 69;
N436	IGR J14515-5542	222.893	-55.681	1.58 ± 0.08	SEYFERT	R 68,46,3; z=0.018;
N437	IGR J14536-5522	223.413	-55.351	1.12 ± 0.08	CV	R 68,110;
N438	IGR J14552-5133	223.849	-51.586	1.18 ± 0.09	SEYFERT	R 70,46; z=0.016;
N439	IGR J14557-5448	223.960	-54.810	0.47 ± 0.08	UNIDENT	
N440	IGR J14561-3738	224.035	-37.640	0.63 ± 0.10	SEYFERT	R 58; z=0.024;
N441	IC 4518A	224.419	-43.129	1.50 ± 0.10	SEYFERT	z=0.016;
N442	IGR J15038-6020	225.960	-60.340	0.75 ± 0.08	CV	R 111;
N443	MRK 841	225.992	10.435	1.96 ± 0.24	SEYFERT	z=0.036;
N444	SWIFT J1508.6-4953	227.163	-49.869	0.92 ± 0.09	BLAZAR	R 112;
N445	IGR J15094-6649	227.363	-66.827	1.72 ± 0.10	CV	R 70,110;
N446	IRAS 15091-2107	227.972	-21.371	1.82 ± 0.22	SEYFERT	z=0.045;
N447	PKS 1510-08	228.210	-9.100	2.25 ± 0.18	BLAZAR	z=0.360;
N448	PSR 1509-58	228.483	-59.143	12.17 ± 0.08	SNR / PULSAR	
N449	SWIFT J1513.8-8125	228.685	-81.386	1.34 ± 0.22	SEYFERT	R 113,15; z=0.068;
N450	4U 1516-569	230.172	-57.167	5.20 ± 0.08	HMXB	
N451	**IGR J15299-2355**	232.480	-23.920	1.05 ± 0.20	UNIDENT	!B16;
N452	IGR J15301-3840	232.540	-38.670	0.90 ± 0.10	AGN	z=0.016;
N453	MCG-01-40-001	233.326	-8.724	1.83 ± 0.17	SEYFERT	z=0.023;
N454	IGR J15335-5420	233.390	-54.340	0.52 ± 0.08	UNIDENT	R 114; !B16; T;
N455	IGR J15360-5750	234.015	-57.811	1.16 ± 0.08	AGN	R 70,115; z=0.023;
N456	SWIFT J1539.2-6227	234.760	-62.430	0.40 ± 0.09	LMXB	R 116,117; T;
N457	IGR J15414-5030	235.369	-50.502	0.62 ± 0.08	SEYFERT	R 100; z=0.032;
N458	4U 1538-522	235.596	-52.385	21.09 ± 0.08	HMXB	
N459	4U 1543-624	236.956	-62.566	3.82 ± 0.10	LMXB	
N460	NY Lup	237.057	-45.480	5.97 ± 0.08	CV	
N461	NGC 5995	237.089	-13.738	2.83 ± 0.13	SEYFERT	z=0.025;

Continued on next page

Table A1 – continued from previous page

Id	Name[1]	RA[2] (deg)	Dec[2] (deg)	Flux[3] (17–60 keV)	Type[4]	Notes
N462	1E 1547.0-5408	237.725	-54.306	1.22 ± 0.08	MAGNETAR	
N463	XTE J1550-564	237.757	-56.458	13.83 ± 0.08	LMXB	T;
N464	IGR J15539-6142	238.438	-61.683	0.74 ± 0.10	SEYFERT	R 104,118; z=0.015;
N465	IGR J15549-3740	238.713	-37.665	0.65 ± 0.11	SEYFERT	R 15; z=0.019;
N466	IGR J15550-4306	238.760	-43.110	0.56 ± 0.08	UNIDENT	R 53; !B16;
N467	2S 1553-542	239.454	-54.415	0.37 ± 0.08	HMXB	
N468	T CrB	239.813	25.912	1.38 ± 0.30	CV	
N469	**IGR J16005-4645**	240.130	-46.760	0.37 ± 0.07	AGN?	R 119; !B16;
N470	4U 1556-605	240.336	-60.693	0.50 ± 0.09	LMXB	
N471	IGR J16058-7253	241.477	-72.901	1.24 ± 0.17	SEYFERT	R 120; z=0.090; AGN pair;
N472	**IGR J16113-4200**	242.827	-42.015	0.41 ± 0.08	UNIDENT	!B16;
N473	IGR J16120-3543	242.974	-35.754	1.76 ± 0.11	AGN?	R 111;
N474	WKK 6092	242.985	-60.624	1.47 ± 0.10	SEYFERT	z=0.016;
N475	4U 1608-52	243.177	-52.422	20.97 ± 0.07	LMXB	
N476	**IGR J16138+1043**	243.470	10.720	1.53 ± 0.34	UNIDENT	!B16;
N477	AT2018cow	244.000	22.270	1.58 ± 0.30	SUPERNOVA	R 121; z=0.014; !B16; T;
N478	IGR J16167-4957	244.145	-49.981	1.66 ± 0.07	CV	R 122,123;
N479	IGR J16173-5023	244.353	-50.363	0.52 ± 0.07	UNIDENT	
N480	PSR J1617-5055	244.364	-50.939	0.63 ± 0.07	SNR / PULSAR	
N481	3C 332.0	244.427	32.376	0.91 ± 0.17	SEYFERT	z=0.151; !B16;
N482	IGR J16181-5407	244.530	-54.120	0.46 ± 0.08	AGN	R 77,111;
N483	IGR J16185-5928	244.624	-59.459	1.17 ± 0.09	SEYFERT	R 70,46; z=0.035;
N484	IGR J16195-2807	244.878	-28.146	2.66 ± 0.16	LMXB	R 54,124;
N485	IGR J16195-4945	244.891	-49.743	2.05 ± 0.07	HMXB	R 122,125;
N486	Sco X-1	244.980	-15.641	861.29 ± 0.11	LMXB	
N487	MAXI J1621-501	245.092	-50.020	0.97 ± 0.07	LMXB	!B16; T;
N488	IGR J16207-5129	245.187	-51.508	3.68 ± 0.07	HMXB	R 122,125;
N489	**IGR J16267-3303**	246.700	-33.060	0.53 ± 0.12	UNIDENT	!B16;
N490	4U 1624-49	247.004	-49.206	3.79 ± 0.07	LMXB	
N491	IGR J16283-4838	247.068	-48.654	0.60 ± 0.07	HMXB	R 126,127;
N492	IGR J16287-5021	247.120	-50.369	0.57 ± 0.07	LMXB	R 15;
N493	IGR J16293-4603	247.311	-46.076	0.44 ± 0.07	LMXB	R 128,129;
N494	IRAS 16288+3929	247.679	39.379	0.79 ± 0.14	SEYFERT	z=0.031;
N495	MAXI J1631-479	247.809	-47.807	12.36 ± 0.07	LMXB?	R 130; C;
N496	IGR J16318-4848	247.951	-48.816	30.69 ± 0.07	HMXB	R 131,132;
N497	IGR J16320-4751	248.008	-47.876	20.99 ± 0.07	HMXB	R 133,134,135,136,137; C;
N498	4U 1626-67	248.073	-67.465	25.78 ± 0.16	LMXB	
N499	4U 1630-47	248.524	-47.390	19.02 ± 0.07	LMXB	
N500	ESO 137-G34	248.807	-58.089	1.54 ± 0.09	SEYFERT	z=0.009;
N501	IGR J16358-4726	248.992	-47.407	0.60 ± 0.07	LMXB	R 138,139;
N502	Triangulum A	249.554	-64.368	1.22 ± 0.14	CLUSTER	z=0.051;
N503	IGR J16385-2057	249.643	-20.914	0.91 ± 0.12	SEYFERT	R 1; z=0.027;
N504	AX J163904-4642	249.773	-46.704	5.85 ± 0.07	HMXB	R 140;
N505	4U 1636-53	250.230	-53.754	34.86 ± 0.08	LMXB	
N506	IGR J16413-4046	250.331	-40.794	0.57 ± 0.07	AGN?	R 16;
N507	IGR J16418-4532	250.455	-45.538	5.03 ± 0.07	HMXB	R 141,135;
N508	GX 340+0	251.449	-45.612	33.16 ± 0.07	LMXB	
N509	IGR J16459-2325	251.480	-23.430	1.28 ± 0.10	UNIDENT	R 53; !B16;
N510	IGR J16465-4507	251.648	-45.118	1.60 ± 0.07	HMXB	R 142,143;
N511	IGR J16479-4514	252.020	-45.213	5.13 ± 0.07	HMXB	R 144,145,135;
N512	IGR J16482-3036	252.047	-30.580	1.31 ± 0.08	SEYFERT	R 54,73; z=0.031;
N513	IGR J16494-1740	252.350	-17.680	0.79 ± 0.11	SEYFERT	R 11; z=0.023; !B16;
N514	IGR J16493-4348	252.373	-43.823	2.57 ± 0.07	HMXB	R 146,147,148;
N515	IGR J16500-3307	252.481	-33.110	1.47 ± 0.07	CV	R 54,1;
N516	NGC 6230	252.660	4.570	0.99 ± 0.23	SEYFERT	R 149; z=0.032;
N517	NGC 6221	253.080	-59.219	1.75 ± 0.11	SEYFERT	z=0.005; C;
N518	XTE J1652-453	253.085	-45.344	1.32 ± 0.07	LMXB?	R 150; T;
N519	NGC 6240	253.245	2.389	4.00 ± 0.21	SEYFERT	z=0.025;

Table A1 – continued from previous page

Id	Name[1]	RA[2] (deg)	Dec[2] (deg)	Flux[3] (17–60 keV)	Type[4]	Notes
N520	MRK 501	253.473	39.758	5.42 ± 0.13	BLAZAR	z=0.034;
N521	GRO J1655-40	253.499	-39.844	6.60 ± 0.07	LMXB	
N522	IGR J16547-1916	253.685	-19.275	1.19 ± 0.10	CV	R 15,151;
N523	IGR J16560-4958	253.989	-49.967	0.58 ± 0.07	AGN	R 16;
N524	IGR J16558-5203	254.031	-52.077	2.16 ± 0.08	SEYFERT	R 122,46; z=0.054;
N525	IGR J16562-3301	254.085	-33.042	1.66 ± 0.07	BLAZAR	R 152; z=2.400;
N526	Her X-1	254.459	35.343	124.15 ± 0.12	LMXB	
N527	**IGR J16580-3247**	254.520	-32.800	0.31 ± 0.06	UNIDENT	!B16;
N528	SWIFT J1658.2-4242	254.553	-42.698	1.76 ± 0.07	LMXB?	R 153,154; !B16; T;
N529	MAXI J1659-152	254.792	-15.268	10.09 ± 0.12	LMXB	R 155; T;
N530	AX J1700.2-4220	255.078	-42.347	1.72 ± 0.07	HMXB	R 110;
N531	OAO 1657-415	255.203	-41.655	76.39 ± 0.07	HMXB	
N532	XTE J1701-462	255.241	-46.188	2.18 ± 0.07	LMXB	T;
N533	IGR J17009+3559	255.246	35.982	1.20 ± 0.12	AGN	R 156,15; z=0.113;
N534	IGR J17014-4306	255.360	-43.110	0.43 ± 0.07	CV	
N535	XTE J1701-407	255.435	-40.858	5.11 ± 0.07	LMXB	
N536	MXB 1659-298	255.500	-29.960	0.28 ± 0.06	LMXB	R 157; !B16;
N537	GX 339-4	255.705	-48.791	77.25 ± 0.07	LMXB	
N538	IGR J17036+3734	255.892	37.567	0.52 ± 0.12	SEYFERT	R 57; z=0.065; !B16;
N539	4U 1700-37	255.982	-37.842	243.43 ± 0.06	HMXB	
N540	IGR J17040-4305	256.010	-43.080	0.36 ± 0.07	CV?	R 93; !B16;
N541	GX 349+2	256.432	-36.422	42.50 ± 0.06	LMXB	
N542	4U 1702-429	256.564	-43.037	18.66 ± 0.07	LMXB	
N543	IGR J17062-6143	256.579	-61.698	2.26 ± 0.15	LMXB	R 158,159,159;
N544	1RXS J170849.0-400910	257.198	-40.154	1.49 ± 0.06	MAGNETAR	
N545	4U 1705-32	257.225	-32.320	1.28 ± 0.06	LMXB	
N546	4U 1705-44	257.227	-44.101	19.61 ± 0.07	LMXB	
N547	IGR J17091-3624	257.289	-36.405	9.75 ± 0.06	LMXB	R 160,161,162,136;
N548	XTE J1709-267	257.388	-26.656	1.18 ± 0.06	LMXB	
N549	IGR J17098-2344	257.450	-23.750	0.54 ± 0.06	SEYFERT	R 11; z=0.036; !B16;
N550	IGR J17098-3628	257.485	-36.448	5.15 ± 0.06	LMXB	R 163,164;
N551	XTE J1710-281	257.550	-28.126	3.28 ± 0.06	LMXB	
N552	RX J1713.7-3946A	257.940	-39.543	0.61 ± 0.06	SNR	R 165; !B16; E;
N553	IGR J17118-3155	257.959	-31.927	0.27 ± 0.05	UNIDENT	
N554	RX J1713.7-3946B	258.047	-39.941	0.68 ± 0.06	SNR	R 165; !B16; E;
N555	4U1708-40	258.111	-40.857	0.66 ± 0.06	LMXB	
N556	Oph cluster	258.113	-23.349	4.10 ± 0.06	CLUSTER	z=0.028; E;
N557	V2400 Oph	258.150	-24.242	3.37 ± 0.06	CV	
N558	SAX J1712.6-3739	258.159	-37.642	6.55 ± 0.06	LMXB	
N559	IGR J17157-5449	258.940	-54.820	0.48 ± 0.10	AGN?	R 166; !B16;
N560	IGR J17158-2124	258.960	-21.410	0.43 ± 0.07	UNIDENT	R 53; !B16;
N561	**IGR J17162-2117**	259.070	-21.290	0.47 ± 0.07	UNIDENT	!B16; C; H;
N562	**IGR J17163-2155**	259.088	-21.917	0.33 ± 0.06	UNIDENT	!B16; C; H;
N563	IGR J17164-3803	259.120	-38.060	0.89 ± 0.06	CV	R 167; !B16;
N564	NGC 6300	259.256	-62.822	5.51 ± 0.17	SEYFERT	z=0.004;
N565	IGR J17174-2436	259.360	-24.610	0.70 ± 0.06	UNIDENT	R 168; !B16;
N566	RX J1718.4-4029	259.611	-40.518	0.38 ± 0.06	LMXB	!B16;
N567	**IGR J17188-3008**	259.720	-30.140	0.31 ± 0.05	UNIDENT	!B16; C;
N568	ARP 102B	259.780	49.020	2.01 ± 0.31	SEYFERT	z=0.024;
N569	GRS 1716-249	259.904	-25.018	1.01 ± 0.05	LMXB	!B16; T;
N570	IGR J17195-4100	259.905	-41.016	2.23 ± 0.06	CV	R 122,110;
N571	IGR J17197-3010	259.928	-30.180	0.22 ± 0.05	LMXB	R 169; !B16;
N572	XTE J1720-318	259.978	-31.748	0.63 ± 0.05	LMXB	
N573	IGR J17200-3116	260.023	-31.293	2.31 ± 0.05	HMXB	R 122,46,76;
N574	IGR J17204-3554	260.073	-35.901	0.55 ± 0.05	AGN	R 54,170;
N575	**IGR J17217-4557**	260.430	-45.960	0.35 ± 0.08	UNIDENT	!B16;
N576	**IGR J17227+3411**	260.690	34.200	0.77 ± 0.14	AGN?	R 171; !B16;
N577	**IGR J17231-3628**	260.780	-36.470	0.30 ± 0.05	UNIDENT	!B16;

Continued on next page

Table A1 – continued from previous page

Id	Name[1]	RA[2] (deg)	Dec[2] (deg)	Flux[3] (17–60 keV)	Type[4]	Notes
N578	IGR J17233-2837	260.849	-28.619	0.81 ± 0.05	SNR / PULSAR	!B16;
N579	IRAS 17216+3633	260.887	36.522	1.38 ± 0.14	SEYFERT	z=0.040;
N580	EXO 1722-363	261.295	-36.281	9.40 ± 0.05	HMXB	
N581	IGR J17254-3257	261.350	-32.963	1.76 ± 0.05	LMXB	R 122,172;
N582	IGR J17255-4509	261.380	-45.170	0.44 ± 0.08	AGN	R 53; !B16;
N583	4U 1724-30	261.885	-30.801	19.06 ± 0.05	LMXB	
N584	IGR J17285-2922	262.171	-29.382	0.22 ± 0.05	LMXB	R 122,173,174;
N585	SWIFT J1728.9-3613	262.232	-36.237	1.11 ± 0.05	LMXB?	R 175; !B16;
N586	1H 1726-058	262.589	-5.981	4.35 ± 0.14	CV	R 122,176;
N587	**IGR J17303-2750**	262.590	-27.840	0.21 ± 0.05	UNIDENT	!B16;
N588	IGR J17306-2015	262.650	-20.260	1.32 ± 0.06	UNIDENT	R 168; !B16;
N589	IGR J17315-3221	262.890	-32.360	0.21 ± 0.05	UNIDENT	R 168; !B16;
N590	GX 9+9	262.937	-16.955	10.48 ± 0.08	LMXB	
N591	GX 354-0	262.987	-33.832	57.58 ± 0.05	LMXB	
N592	V2487 Oph	263.008	-19.206	0.72 ± 0.07	CV	
N593	GX 1+4	263.011	-24.743	69.52 ± 0.05	LMXB	
N594	IGR J17327-4405	263.190	-44.100	0.58 ± 0.08	UNIDENT	R 53; !B16;
N595	IGR J17329-2731	263.227	-27.531	0.63 ± 0.04	LMXB	R 177; !B16;
N596	IGR J17331-2406	263.248	-24.143	0.38 ± 0.05	LMXB?	R 178,115; T;
N597	Rapid Burster	263.348	-33.392	3.61 ± 0.05	LMXB	
N598	**IGR J17342-4049**	263.570	-40.830	0.30 ± 0.06	UNIDENT	!B16;
N599	SWIFT J1734.5-3027	263.620	-30.380	0.85 ± 0.04	LMXB	R 179; !B16;
N600	IGR J17350-2045	263.740	-20.748	0.79 ± 0.06	SEYFERT	R 89,47; z=0.044;
N601	**IGR J17350-1957**	263.750	-19.960	0.32 ± 0.06	UNIDENT	!B16;
N602	IGR J17353-3539	263.844	-35.657	0.57 ± 0.05	LMXB	R 180;
N603	IGR J17353-3257	263.857	-32.922	1.31 ± 0.05	HMXB	R 181,100,182;
N604	IGR J17361-4444	264.040	-44.730	0.61 ± 0.08	LMXB?	R 183,184,185; T;
N605	GRS 1734-292	264.368	-29.133	6.43 ± 0.04	SEYFERT	z=0.021;
N606	ESO 139-G012	264.480	-59.950	1.15 ± 0.16	SEYFERT	z=0.017;
N607	**IGR J17381-2345**	264.530	-23.750	0.23 ± 0.05	UNIDENT	!B16;
N608	SLX 1735-269	264.571	-26.991	15.87 ± 0.04	LMXB	
N609	4U 1735-444	264.745	-44.451	21.54 ± 0.08	LMXB	
N610	IGR J17391-3021	264.805	-30.344	0.99 ± 0.04	HMXB	R 186,187,188;
N611	GRS 1736-297	264.876	-29.703	0.66 ± 0.04	LMXB	
N612	XTE J1739-285	264.975	-28.496	1.22 ± 0.04	LMXB	
N613	AX J1740.3-2904	265.030	-29.040	0.24 ± 0.04	CV	
N614	AX J1740.1-2847	265.060	-28.820	0.34 ± 0.04	CV	R 189; !B16;
N615	IGR J17402-3656	265.092	-36.920	0.65 ± 0.05	CV	R 100,77;
N616	SLX 1737-282	265.168	-28.313	4.31 ± 0.04	LMXB	
N617	IGR J17407-2808	265.175	-28.133	1.88 ± 0.04	HMXB	R 190,191;
N618	IGR J17418-1212	265.483	-12.198	2.02 ± 0.10	SEYFERT	R 192,193; z=0.037;
N619	IGR J17422-2108	265.560	-21.140	0.24 ± 0.05	SEYFERT	R 11; z=0.106; !B16;
N620	GRS 1739-278	265.650	-27.780	2.47 ± 0.04	LMXB	!B16; T;
N621	XTE J1743-363	265.748	-36.380	1.29 ± 0.05	HMXB	R 194;
N622	PKS 1741-03	265.970	-3.788	0.59 ± 0.12	BLAZAR	z=1.054;
N623	1E 1740.7-294	265.984	-29.735	50.02 ± 0.04	LMXB	
N624	GRO J1744-28	266.138	-28.741	3.80 ± 0.04	LMXB	
N625	IGR J17446-2947	266.174	-29.805	12.13 ± 0.04	LMXB	R 195,196,197; T; C;
N626	**IGR J17449-3037**	266.230	-30.620	0.21 ± 0.04	UNIDENT	!B16;
N627	KS 1741-293	266.242	-29.337	6.40 ± 0.04	LMXB	T;
N628	GRS 1741.9-2853	266.250	-28.917	4.45 ± 0.04	LMXB	R 198,103; T;
N629	SWIFT J174510.8-262411	266.295	-26.404	0.48 ± 0.04	LMXB?	R 199; !B16; T;
N630	IGR J17456-2901	266.401	-29.026	6.99 ± 0.04	GAL CENTER	R 200,201,202; SGR A*; C;
N631	SWIFT J1745.4+2906	266.460	29.140	1.01 ± 0.22	SEYFERT	R 203; z=0.111; !B16;
N632	A 1742-294	266.525	-29.518	11.77 ± 0.04	LMXB	R 204; T;
N633	IGR J17464-3213	266.564	-32.234	25.26 ± 0.04	LMXB	R 205,206; T;
N634	1E 1743.1-2843	266.580	-28.735	6.14 ± 0.04	LMXB	
N635	SAX J1747.0-2853	266.761	-28.883	4.45 ± 0.04	LMXB	R 207,208; T;

Table A1 – continued from previous page

Id	Name[1]	RA[2] (deg)	Dec[2] (deg)	Flux[3] (17–60 keV)	Type[4]	Notes
N636	IGR J17464-2811	266.817	-28.180	1.37 ± 0.04	LMXB	R 209,210,211,212,208; T;
N637	SLX 1744-299/300	266.834	-30.010	8.94 ± 0.04	LMXB	T;
N638	IGR J17473-2721	266.838	-27.348	1.78 ± 0.04	LMXB	R 213,214,215,216,217; T;
N639	IGR J17475-2822	266.868	-28.370	2.12 ± 0.04	MOL CLOUD	R 218,219,220;
N640	IGR J17475-2253	266.886	-22.872	0.86 ± 0.05	SEYFERT	R 87,98,221; z=0.047;
N641	IGR J17479-2807	266.982	-28.121	1.06 ± 0.04	LMXB	R 14,52;
N642	GX 3+1	266.984	-26.556	11.59 ± 0.04	LMXB	
N643	IGR J17488-2338	267.150	-23.590	0.22 ± 0.05	SEYFERT	R 67; z=0.240;
N644	4U 1745-203	267.208	-20.361	0.97 ± 0.06	LMXB	T;
N645	IGR J17488-3253	267.218	-32.920	1.37 ± 0.04	SEYFERT	R 122,46,222; z=0.020;
N646	AX J1749.1-2733	267.275	-27.550	0.98 ± 0.04	HMXB	R 223,224; T;
N647	AX J1749.2-2725	267.292	-27.421	0.54 ± 0.04	HMXB	R 225,226,227;
N648	GRO J1750-27	267.300	-26.647	4.29 ± 0.04	HMXB	R 228,229; T;
N649	IGR J17497-2821	267.396	-28.353	1.89 ± 0.04	LMXB	R 230,231,232;
N650	IGR J17498-2921	267.482	-29.323	0.53 ± 0.04	LMXB	R 233,234,235,236,237,238; !B16; T;
N651	4U 1746-37	267.552	-37.046	2.44 ± 0.05	LMXB	
N652	SAX J1750.8-2900	267.600	-29.038	2.25 ± 0.04	LMXB	C;
N653	IGR J17505-2644	267.658	-26.734	0.69 ± 0.04	LMXB?	R 239,240;
N654	IGR J17507-2856	267.683	-28.922	1.43 ± 0.04	UNIDENT	R 241,3,242; T; C;
N655	GRS 1747-312	267.691	-31.282	1.45 ± 0.04	LMXB	R 243; T;
N656	IGR J17513-2011	267.824	-20.197	1.28 ± 0.06	SEYFERT	R 54,46; z=0.047;
N657	SWIFT J1751.8-6019	267.968	-60.322	1.14 ± 0.17	SEYFERT	R 22; z=0.112;
N658	XTE J1752-223	268.044	-22.325	0.86 ± 0.05	LMXB	
N659	IGR J17528-2022	268.210	-20.370	0.31 ± 0.06	CV?	R 244; !B16;
N660	SWIFT J1753.5-0127	268.368	-1.452	81.97 ± 0.11	LMXB	R 245,246; T;
N661	AX J1753.5-2745	268.375	-27.750	0.21 ± 0.04	UNIDENT	R 77; !B16;
N662	SAX J1753.5-2349	268.400	-23.810	0.21 ± 0.05	LMXB	R 247;
N663	IGR J17538-2544	268.460	-25.750	0.20 ± 0.04	UNIDENT	R 248,249,250; !B16; T; H;
N664	AX J1754.2-2754	268.574	-27.902	0.29 ± 0.04	LMXB	R 251,247; !B16;
N665	IGR J17544-2619	268.601	-26.321	0.76 ± 0.04	HMXB	R 252,253; T;
N666	**IGR J17554-1832**	268.860	-18.550	0.29 ± 0.06	UNIDENT	!B16;
N667	IGR J17570-2500	269.270	-25.020	0.38 ± 0.05	UNIDENT	R 53; !B16; H;
N668	IGR J17585-3057	269.615	-30.960	0.56 ± 0.04	LMXB?	R 254;
N669	IGR J17586-2129	269.656	-21.372	1.80 ± 0.05	CV?	R 100,69,76,77,76;
N670	IGR J17591-2342	269.787	-23.713	0.96 ± 0.05	LMXB	R 255,256; !B16; T;
N671	IGR J17596-2315	269.910	-23.270	0.47 ± 0.05	UNIDENT	R 53; !B16;
N672	IGR J17597-2201	269.939	-22.019	2.40 ± 0.05	LMXB	R 257,258,135,208,76;
N673	**IGR J17597-1935**	269.940	-19.600	0.29 ± 0.06	UNIDENT	!B16;
N674	**IGR J17598-2236**	269.950	-22.600	0.29 ± 0.05	UNIDENT	!B16;
N675	NGC 6552	270.030	66.615	0.71 ± 0.12	SEYFERT	z=0.027;
N676	**IGR J18006-3426**	270.170	-34.450	0.25 ± 0.05	UNIDENT	!B16;
N677	V2301 OPH	270.170	8.181	1.47 ± 0.16	CV	
N678	IGR J18007-4146	270.230	-41.810	0.79 ± 0.08	CV	R 111,56,259;
N679	IGR J18010-3045	270.270	-30.760	0.37 ± 0.04	UNIDENT	R 53,93; !B16;
N680	GX 5-1	270.286	-25.078	48.68 ± 0.05	LMXB	
N681	GRS 1758-258	270.302	-25.743	74.70 ± 0.05	LMXB	
N682	GX 9+1	270.387	-20.517	17.21 ± 0.06	LMXB	C;
N683	IGR J18017-3542	270.440	-35.710	2.16 ± 0.05	CV?	R 53,93; !B16;
N684	IGR J18027-2016	270.677	-20.278	5.33 ± 0.06	HMXB	R 260,261; T; C;
N685	IGR J18027-1455	270.692	-14.907	2.14 ± 0.07	SEYFERT	R 122,262; z=0.036;
N686	1RXS J180408.9-342058	271.038	-34.349	3.57 ± 0.05	LMXB	R 263; !B16; T;
N687	IGR J18044-2739	271.110	-27.660	0.77 ± 0.04	CV	R 264,265;
N688	IGR J18044-1829	271.110	-18.490	0.46 ± 0.06	UNIDENT	R 11; !B16;
N689	IGR J18048-1455	271.177	-14.942	0.76 ± 0.07	CV	R 54,89;
N690	SAX J1806.5-2215	271.642	-22.252	2.72 ± 0.05	LMXB	R 266,267,268,212; !B16;
N691	XTE J1807-294	271.744	-29.416	0.58 ± 0.05	LMXB	T;
N692	IGR J18070-3507	271.760	-35.130	0.30 ± 0.05	UNIDENT	R 53; !B16;
N693	IGR J18078+1123	271.946	11.381	1.22 ± 0.17	SEYFERT	R 15; z=0.079;

Continued on next page

Table A1 – continued from previous page

Id	Name[1]	RA[2] (deg)	Dec[2] (deg)	Flux[3] (17–60 keV)	Type[4]	Notes
N694	V426 Oph	271.973	5.815	0.56 ± 0.13	CV	!B16;
N695	SAX J1808.4-3658	272.115	-36.979	0.56 ± 0.06	LMXB	T;
N696	SGR 1806-20	272.165	-20.411	2.45 ± 0.06	SNR / PULSAR	
N697	IGR J18088-2741	272.210	-27.700	0.67 ± 0.05	CV	R 167,114; !B16;
N698	IGR J18102-1751	272.560	-17.850	0.65 ± 0.07	UNIDENT	R 53; !B16;
N699	XTE J1810-189	272.585	-19.070	2.97 ± 0.06	LMXB	T;
N700	SAX J1810.8-2609	272.685	-26.150	1.82 ± 0.05	LMXB	
N701	IGR J18109-2631	272.740	-26.520	0.42 ± 0.05	UNIDENT	R 53; !B16; C;
N702	IGR J18112-2641	272.820	-26.690	0.47 ± 0.05	CV?	R 53,93; !B16;
N703	PSR J1811-1925	272.862	-19.420	1.16 ± 0.06	SNR / PULSAR	
N704	MAXI J1810-222	273.170	-22.310	0.39 ± 0.06	LMXB	R 269; !B16; T;
N705	IGR J18134-1636	273.364	-16.618	0.76 ± 0.07	AGN?	R 208;
N706	MAXI J1813-095	273.392	-9.533	0.36 ± 0.08	LMXB	R 270,271,272; !B16;
N707	IGR J18135-1751	273.397	-17.841	1.76 ± 0.07	SNR / PULSAR	R 273,274;
N708	IGR J18141-1823	273.540	-18.390	0.51 ± 0.07	AGN?	R 11; !B16;
N709	IGR J18141-0606	273.550	-6.110	0.46 ± 0.08	UNIDENT	R 53; !B16;
N710	GX 13+1	273.629	-17.155	13.09 ± 0.07	LMXB	
N711	IGR J18147-3400	273.690	-34.010	0.56 ± 0.05	UNIDENT	R 53; !B16;
N712	**IGR J18149-2247**	273.740	-22.800	0.26 ± 0.06	UNIDENT	!B16;
N713	4U 1812-12	273.777	-12.094	35.46 ± 0.08	LMXB	
N714	IGR J18151-1052	273.778	-10.879	0.54 ± 0.08	CV	R 156,275,276;
N715	GX 17+2	274.006	-14.035	62.73 ± 0.07	LMXB	
N716	AM Her	274.041	49.872	6.18 ± 0.54	CV	
N717	IGR J18165-3912	274.140	-39.200	0.63 ± 0.08	CV?	R 78; !B16;
N718	SWIFT J1816.7-1613	274.141	-16.252	0.29 ± 0.07	HMXB	R 277,278; T;
N719	IGR J18170-2511	274.310	-25.152	1.37 ± 0.05	CV	R 7;
N720	IGR J18172-1944	274.310	-19.740	0.50 ± 0.06	UNIDENT	R 53; !B16; T;
N721	XTE J1817-330	274.431	-33.019	3.40 ± 0.05	LMXB	T;
N722	XTE J1818-245	274.606	-24.528	3.18 ± 0.05	LMXB	
N723	IGR J18184-2352	274.610	-23.880	0.88 ± 0.06	CV?	R 53; !B16;
N724	SAX J1818.6-1703	274.679	-17.041	1.60 ± 0.07	HMXB	R 1; T;
N725	IGR J18193-2542	274.880	-25.680	0.64 ± 0.05	UNIDENT	R 3; !B16;
N726	MAXI J1820+070	275.091	7.185	16.25 ± 0.11	LMXB	R 279; !B16; T;
N727	AX J1820.5-1434	275.133	-14.564	1.41 ± 0.07	HMXB	
N728	IGR J18214-1318	275.327	-13.316	1.68 ± 0.08	HMXB	R 54,280,281,282; T;
N729	IGR J18219-1347	275.498	-13.792	0.74 ± 0.08	HMXB	R 89,283;
N730	H 1821+643	275.506	64.369	1.53 ± 0.13	SEYFERT	
N731	4U 1820-30	275.918	-30.365	35.61 ± 0.06	LMXB	
N732	IC 4709	276.086	-56.376	2.85 ± 0.18	SEYFERT	z=0.017;
N733	XTE J1824-141	276.115	-14.438	0.88 ± 0.08	HMXB?	R 284,77;
N734	IGR J18245-2452	276.140	-24.880	1.02 ± 0.06	LMXB	R 285; !B16; T;
N735	IGR J18249-3243	276.225	-32.734	1.02 ± 0.06	SEYFERT	R 286,7,287; z=0.355;
N736	4U 1823-00	276.335	0.000	1.91 ± 0.09	LMXB	
N737	IGR J18256-1035	276.443	-10.589	0.75 ± 0.08	HMXB	R 3,67,77,208;
N738	4U 1822-371	276.445	-37.106	29.71 ± 0.07	LMXB	
N739	IGR J18257-0707	276.486	-7.155	0.95 ± 0.08	SEYFERT	R 54,3; z=0.037;
N740	IGR J18263-1345	276.550	-13.694	0.55 ± 0.08	UNIDENT	R 53; !B16;
N741	LS 5039	276.557	-14.855	1.09 ± 0.08	HMXB	
N742	IGR J18284-0229	277.110	-2.480	0.37 ± 0.08	UNIDENT	R 52;
N743	MAXI J1828-249	277.243	-25.030	1.06 ± 0.06	LMXB	R 288,289; !B16; T;
N744	IGR J18293-1213	277.340	-12.222	0.59 ± 0.08	CV?	R 290,63,89;
N745	GS 1826-24	277.370	-23.798	93.74 ± 0.06	LMXB	
N746	**IGR J18303-3345**	277.592	-33.752	0.55 ± 0.07	UNIDENT	!B16; C; H;
N747	AX J1830.6-1002	277.650	-10.047	0.81 ± 0.08	AGN?	R 291;
N748	IGR J18308-1232	277.698	-12.531	0.85 ± 0.08	CV	R 100;
N749	IGR J18308+0928	277.710	9.480	0.47 ± 0.09	SEYFERT	R 15; z=0.019;
N750	IGR J18312-3334	277.820	-33.580	0.63 ± 0.07	SEYFERT	R 52,15;
N751	AX J1832.3-0840	278.109	-8.660	0.69 ± 0.08	CV	

<div align="right">Continued on next page</div>

Table A1 – continued from previous page

Id	Name[1]	RA[2] (deg)	Dec[2] (deg)	Flux[3] (17–60 keV)	Type[4]	Notes
N752	IGR J18325-0756	278.110	-7.944	1.19 ± 0.08	HMXB?	R 292,3;
N753	SNR 021.5-00.9	278.388	-10.583	4.00 ± 0.08	SNR / PULSAR	
N754	PKS 1830-211	278.421	-21.056	3.07 ± 0.07	BLAZAR	z=2.507;
N755	3C 382	278.783	32.698	4.13 ± 0.30	SEYFERT	z=0.058;
N756	MAXI J1836-194	278.931	-19.320	2.51 ± 0.08	LMXB	R 293; !B16; T;
N757	RX J1832-33	278.931	-32.993	7.94 ± 0.07	LMXB	
N758	FAIRALL 49	279.210	-59.410	1.04 ± 0.19	SEYFERT	z=0.020;
N759	AX J1838.0-0655	279.505	-6.918	2.74 ± 0.08	SNR / PULSAR	R 294;
N760	IGR J18381-0924	279.534	-9.414	0.66 ± 0.08	SEYFERT?	R 167,114; z=0.031;
N761	ESO 103-G035	279.576	-65.425	6.16 ± 0.22	SEYFERT	z=0.013;
N762	SWIFT J1839.1-5717	279.761	-57.296	1.03 ± 0.19	UNIDENT	R 56,295;
N763	Ser X-1	279.991	5.041	11.28 ± 0.07	LMXB	
N764	IGR J18400-2439	280.020	-24.660	0.33 ± 0.08	UNIDENT	R 168; !B16;
N765	IGR J18410-0535	280.255	-5.573	1.11 ± 0.08	HMXB	R 296,297;
N766	1E 1841-045	280.333	-4.941	3.47 ± 0.08	MAGNETAR	
N767	3C 390.3	280.582	79.768	5.01 ± 0.21	SEYFERT	z=0.056;
N768	IGR J18434-0508	280.860	-5.140	0.49 ± 0.08	CV?	R 53,93; !B16;
N769	ESO 140-G043	281.212	-62.376	2.83 ± 0.20	SEYFERT	z=0.014;
N770	AX J1845.0-0433	281.267	-4.568	1.73 ± 0.08	HMXB	
N771	GS 1843+00	281.404	0.872	3.84 ± 0.07	HMXB	T;
N772	SWIFT J1845.7-0037	281.478	-0.659	0.42 ± 0.07	HMXB	R 298,299,300,301; !B16;
N773	IGR J18462-0223	281.567	-2.387	0.31 ± 0.07	HMXB	R 302,303,304,305;
N774	PSR J1846-0258	281.610	-2.977	2.25 ± 0.08	SNR / PULSAR	R 306;
N775	H 1846-786	281.779	-78.560	1.16 ± 0.22	SEYFERT	z=0.074; !B16;
N776	1A 1845-024	282.062	-2.443	2.15 ± 0.07	HMXB	T;
N777	IGR J18483-0311	282.071	-3.172	5.74 ± 0.08	HMXB	R 307,145,1;
N778	IGR J18486-0047	282.097	-0.777	1.30 ± 0.07	AGN?	R 100;
N779	IGR J18490-0000	282.264	-0.020	1.36 ± 0.07	SNR / PULSAR	R 308,309;
N780	EXO 1846-031	282.321	-3.062	0.65 ± 0.08	LMXB	!B16; C;
N781	IGR J18497-0248	282.446	-2.804	0.57 ± 0.07	UNIDENT	R 310,77; !B16;
N782	4U 1850-08	283.270	-8.706	6.83 ± 0.08	LMXB	
N783	IGR J18538-0102	283.459	-1.034	0.57 ± 0.07	SEYFERT	R 35; z=0.145;
N784	IGR J18544+0839	283.610	8.660	0.50 ± 0.07	AGN?	R 11; !B16;
N785	ESO 025-G002	283.752	-78.891	1.15 ± 0.22	SEYFERT	z=0.029; C;
N786	4U 1849-31	283.762	-31.162	7.85 ± 0.10	CV	
N787	XTE J1855-026	283.876	-2.604	13.01 ± 0.07	HMXB	T;
N788	IGR J18559+1535	283.990	15.635	1.67 ± 0.08	SEYFERT	R 311; z=0.084;
N789	XTE J1856+053	284.179	5.310	0.32 ± 0.06	LMXB	T;
N790	2E 1849.2-7832	284.388	-78.491	1.97 ± 0.22	SEYFERT	z=0.042;
N791	SWIFT J1858.6-0814	284.645	-8.237	0.74 ± 0.09	X-RAY BINARY	!B16; T;
N792	XTE J1858+034	284.693	3.430	5.72 ± 0.06	HMXB	T;
N793	XTE J1859+083	284.775	8.250	0.60 ± 0.06	HMXB	!B16;
N794	HETE J19001-2455	285.036	-24.920	22.99 ± 0.12	LMXB	R 312; T;
N795	XTE J1901+014	285.419	1.444	3.85 ± 0.07	LMXB?	R 313,314,261; T;
N796	4U 1901+03	285.914	3.215	12.96 ± 0.06	HMXB	T;
N797	IGR J19039+3348	285.985	33.815	1.14 ± 0.15	SEYFERT	R 33; z=0.015; !B16;
N798	IGR J19071+0716	286.780	7.270	0.25 ± 0.06	UNIDENT	R 53; !B16;
N799	V1082 Sgr	286.807	-20.765	1.14 ± 0.13	CV?	R 315;
N800	SGR 1900+14	286.848	9.322	1.09 ± 0.06	MAGNETAR	
N801	IGR J19077-3925	286.900	-39.378	0.87 ± 0.11	SEYFERT	R 15; z=0.073;
N802	XTE J1908+094	287.221	9.385	0.58 ± 0.06	LMXB	
N803	SWIFT J1909.3+0124	287.340	1.200	0.34 ± 0.07	CV	R 316,317; !B16;
N804	4U 1907+09	287.407	9.832	13.66 ± 0.06	HMXB	T;
N805	4U 1909+07	287.701	7.599	17.82 ± 0.06	HMXB	
N806	Aql X-1	287.814	0.584	10.06 ± 0.07	LMXB	T;
N807	IGR J19113+1413	287.830	14.220	0.79 ± 0.07	CV	R 77,318; !B16;
N808	SS 433	287.954	4.983	10.59 ± 0.06	HMXB	
N809	IGR J19140+0951	288.518	9.884	11.28 ± 0.06	HMXB	R 319,261;

Table A1 – continued from previous page

Id	Name[1]	RA[2] (deg)	Dec[2] (deg)	Flux[3] (17–60 keV)	Type[4]	Notes
N810	GRS 1915+105	288.798	10.945	315.96 ± 0.06	LMXB	
N811	IGR J19173+0747	289.330	7.830	0.75 ± 0.06	CV?	R 167,320;
N812	4U 1915-05	289.699	-5.237	10.73 ± 0.10	LMXB	
N813	IGR J19193+0754	289.820	7.908	0.28 ± 0.06	UNIDENT	R 321; !B16;
N814	IGR J19194-2956	289.863	-29.959	1.00 ± 0.13	SEYFERT	R 15; z=0.167;
N815	ABELL 2319	290.260	43.974	1.35 ± 0.15	CLUSTER	
N816	ESO141-G055	290.302	-58.678	3.79 ± 0.23	SEYFERT	z=0.037;
N817	SWIFT J1922.7-1716	290.601	-17.297	0.72 ± 0.14	LMXB	R 322,323;
N818	**IGR J19225+1836**	290.640	18.610	0.40 ± 0.08	UNIDENT	!B16;
N819	PKS 1921-293	291.220	-29.246	1.01 ± 0.14	BLAZAR	z=0.352;
N820	IGR J19260+4136	291.578	41.586	0.55 ± 0.12	SEYFERT	R 22; z=0.071; !B16;
N821	SWIFT J1926.4-0501	291.581	-5.020	0.46 ± 0.10	AGN	R 38; !B16;
N822	IGR J19267+1325	291.646	13.396	0.55 ± 0.07	CV	R 324;
N823	IGR J19294+1328	292.360	13.470	0.69 ± 0.07	AGN	R 111;
N824	**IGR J19295-0225**	292.390	-2.420	0.61 ± 0.10	UNIDENT	!B16;
N825	IGR J19294+1816	292.483	18.311	1.47 ± 0.08	HMXB	R 325;
N826	IGR J19302+3411	292.525	34.174	1.20 ± 0.09	SEYFERT	R 24; z=0.063;
N827	SNR G054.1+00.3	292.630	18.860	0.76 ± 0.08	SNR / PULSAR	
N828	SWIFT J1933.9+3258	293.437	32.915	1.43 ± 0.09	SEYFERT	R 326,31; z=0.058;
N829	SWIFT J1937.5-4021	294.310	-40.270	0.50 ± 0.10	UNIDENT	R 38; !B16;
N830	1H 1934-063	294.405	-6.227	1.55 ± 0.13	SEYFERT	z=0.010;
N831	RX J1940.2-1025	295.056	-10.423	3.51 ± 0.15	CV	
N832	IGR J19405-3016	295.065	-30.268	1.43 ± 0.14	SEYFERT	R 1; z=0.052;
N833	IGR J19421+3613	295.530	36.220	0.38 ± 0.08	UNIDENT	R 53; !B16;
N834	NGC 6814	295.674	-10.325	4.10 ± 0.15	SEYFERT	z=0.005;
N835	IGR J19443+2117	296.023	21.305	0.95 ± 0.09	BLAZAR?	R 100;
N836	XTE J1946+274	296.414	27.365	3.06 ± 0.09	HMXB	T;
N837	XSS J19459+4508	296.806	44.823	1.63 ± 0.10	SEYFERT	R 70,45; z=0.054;
N838	IGR J19491-1035	297.280	-10.590	1.01 ± 0.16	SEYFERT	R 41; z=0.024;
N839	KS 1947+300	297.396	30.212	8.65 ± 0.08	HMXB	
N840	AX J1949.8+2534	297.467	25.573	0.64 ± 0.09	HMXB	R 327; !B16;
N841	IGR J19504+3318	297.620	33.310	1.09 ± 0.07	AGN?	R 53,93; !B16;
N842	3C 403	298.096	2.504	0.98 ± 0.11	SEYFERT	z=0.058;
N843	PSR B1951+32	298.250	32.930	1.08 ± 0.07	SNR / PULSAR	
N844	IGR J19552+0044	298.800	0.770	0.70 ± 0.13	CV	R 328;
N845	4U 1954+31	298.925	32.097	12.52 ± 0.07	LMXB	R 329;
N846	IGR J19577+3339	299.440	33.650	0.43 ± 0.07	AGN?	R 53,93; !B16;
N847	V2306 Cyg	299.570	32.551	1.19 ± 0.07	CV	
N848	Cyg X-1	299.590	35.204	867.58 ± 0.07	HMXB	
N849	4U 1957+11	299.809	11.713	1.87 ± 0.11	LMXB	
N850	Cyg A	299.869	40.739	6.49 ± 0.07	SEYFERT	z=0.056;
N851	1ES 1959+650	299.999	65.149	1.33 ± 0.19	BLAZAR	z=0.047;
N852	SWIFT J2000.6+3210	300.093	32.187	1.72 ± 0.07	HMXB	R 330;
N853	IGR J20063+3641	301.576	36.698	0.58 ± 0.07	CV	R 318,244; !B16;
N854	ESO 399-IG 020	301.755	-34.534	1.14 ± 0.13	SEYFERT	z=0.025;
N855	IGR J20084+3221	302.120	32.350	0.69 ± 0.07	CV?	R 53,93; !B16;
N856	NGC 6860	302.184	-61.086	2.41 ± 0.36	SEYFERT	z=0.015;
N857	IGR J20107+4534	302.680	45.570	0.65 ± 0.08	UNIDENT	R 114; !B16;
N858	IGR J20159+3713	303.946	37.213	1.05 ± 0.07	SNR	R 318,331; C;
N859	**IGR J20166+7603**	304.170	76.060	1.26 ± 0.26	UNIDENT	!B16;
N860	**IGR J20169+2714**	304.230	27.230	0.42 ± 0.09	UNIDENT	!B16;
N861	PKS 2014-55	304.466	-55.629	2.08 ± 0.42	SEYFERT	R 22; z=0.060;
N862	IGR J20187+4041	304.642	40.694	1.75 ± 0.07	SEYFERT	R 286,332; z=0.014;
N863	IGR J20216+4359	305.428	44.012	1.00 ± 0.07	SEYFERT	R 333; z=0.017;
N864	V404 Cyg	306.016	33.867	41.78 ± 0.07	HMXB	!B16; T;
N865	IGR J20286+2544	307.143	25.746	3.20 ± 0.11	SEYFERT	R 286,334,335; z=0.014; AGN pair;
N866	IGR J20310+3835	307.755	38.576	0.54 ± 0.07	AGN?	R 111,56;
N867	EXO 2030+375	308.062	37.638	59.10 ± 0.07	HMXB	T;

Continued on next page

Table A1 – continued from previous page

Id	Name[1]	RA[2] (deg)	Dec[2] (deg)	Flux[3] (17–60 keV)	Type[4]	Notes
N868	Cyg X-3	308.108	40.959	181.74 ± 0.07	HMXB	
N869	4C +21.55	308.405	21.791	1.63 ± 0.16	BLAZAR	z=0.174;
N870	SWIFT J2037.2+4151	309.252	41.833	0.60 ± 0.07	UNIDENT	R 77,336,337;
N871	4C +74.26	310.661	75.126	3.51 ± 0.30	SEYFERT	z=0.104;
N872	RX J2044.0+2833	311.004	28.550	1.08 ± 0.11	SEYFERT	z=0.049;
N873	MRK 509	311.043	-10.731	5.16 ± 0.17	SEYFERT	z=0.034;
N874	IC 5063	312.943	-57.056	3.99 ± 0.76	SEYFERT	R 22; z=0.011; !B16;
N875	SWIFT J2055.0+3559	313.770	35.950	0.38 ± 0.08	UNIDENT	R 38; !B16;
N876	IGR J20569+4940	314.178	49.660	0.94 ± 0.08	BLAZAR	R 97,77;
N877	IGR J20596+4303	314.956	43.058	0.46 ± 0.08	UNIDENT	R 22,78; !B16; C;
N878	SAX J2103.5+4545	315.897	45.750	10.44 ± 0.08	HMXB	T;
N879	**IGR J21060-4447**	316.520	-44.780	1.58 ± 0.31	UNIDENT	!B16;
N880	RX J2109.4+3532	317.490	35.560	0.56 ± 0.10	BLAZAR?	z=0.202; !B16;
N881	IGR J21133+3154	318.340	31.947	0.55 ± 0.13	STAR	!B16;
N882	1RXS J211336.1+542226	318.375	54.368	0.46 ± 0.09	CV	R 15;
N883	S5 2116+81	318.624	82.077	2.16 ± 0.39	SEYFERT	z=0.086;
N884	IGR J21178+5139	319.464	51.650	1.51 ± 0.09	BLAZAR?	R 286,338; z=0.002;
N885	IGR J21196+3333	319.899	33.552	1.16 ± 0.13	SEYFERT	R 15; z=0.051;
N886	RX J2123.7+4217	320.920	42.296	1.33 ± 0.09	CV	
N887	IGR J21247+5058	321.163	50.975	10.56 ± 0.09	SEYFERT	R 122,262; z=0.015;
N888	IGR J21277+5656	321.922	56.937	2.92 ± 0.10	SEYFERT	R 311; z=0.015;
N889	4U 2129+12	322.489	12.175	4.81 ± 0.40	LMXB	
N890	RX J2133.7+5107	323.433	51.132	3.77 ± 0.09	CV	R 123;
N891	IGR J21358+4729	323.976	47.486	1.49 ± 0.09	SEYFERT	z=0.025;
N892	IGR J21382+3204	324.582	32.036	1.13 ± 0.21	SEYFERT	R 22; z=0.025; !B16;
N893	IGR J21397+5949	324.905	59.848	0.83 ± 0.11	SEYFERT	R 15; z=0.114;
N894	SS Cyg	325.688	43.577	3.43 ± 0.10	CV	
N895	Cyg X-2	326.170	38.319	28.13 ± 0.14	LMXB	
N896	PKS 2149-306	327.981	-30.465	3.69 ± 0.18	BLAZAR	R 339; z=2.345;
N897	MRK 520	330.124	10.547	2.18 ± 0.39	SEYFERT	R 340; z=0.027;
N898	IGR J22018+5049	330.471	50.810	0.80 ± 0.10	BLAZAR	R 22; z=1.899; !B16;
N899	NGC 7172	330.490	-31.877	7.55 ± 0.18	SEYFERT	z=0.009;
N900	BL Lac	330.672	42.281	1.35 ± 0.14	BLAZAR	z=0.069;
N901	4U 2206+54	331.987	54.518	9.99 ± 0.10	HMXB	T;
N902	FO Aqr	334.481	-8.351	2.68 ± 0.48	CV	
N903	SWIFT J2221.6+5952	335.540	59.880	0.47 ± 0.09	UNIDENT	R 38; !B16;
N904	IGR J22292+6646	337.324	66.778	0.89 ± 0.09	SEYFERT	R 15; z=0.112;
N905	NGC 7314	338.940	-26.061	3.34 ± 0.25	SEYFERT	z=0.005;
N906	MRK 915	339.155	-12.531	2.34 ± 0.32	SEYFERT	z=0.024; !B16;
N907	3C 452	341.383	39.683	2.21 ± 0.44	SEYFERT	z=0.081;
N908	**IGR J22516+5610**	342.900	56.180	0.38 ± 0.08	UNIDENT	!B16;
N909	IGR J22517+2218	342.939	22.316	1.30 ± 0.20	BLAZAR	R 341; z=3.668;
N910	IGR J22534+6243	343.350	62.720	0.58 ± 0.07	HMXB	R 342,343,344; !B16;
N911	3C 454.3	343.490	16.146	9.01 ± 0.17	BLAZAR	z=0.859;
N912	MR 2251-178	343.507	-17.604	1.96 ± 0.28	SEYFERT	z=0.064;
N913	AX J2254.3+1146	343.610	11.760	0.83 ± 0.19	SEYFERT	z=0.028; !B16;
N914	AO Psc	343.837	-3.164	1.97 ± 0.43	CV	
N915	Kaz 320	344.874	24.917	1.94 ± 0.23	SEYFERT	z=0.035;
N916	NGC 7465	345.508	15.953	1.35 ± 0.17	SEYFERT	z=0.007;
N917	NGC 7469	345.837	8.870	4.34 ± 0.23	SEYFERT	z=0.016;
N918	MRK 926	346.176	-8.685	4.10 ± 0.32	SEYFERT	z=0.047;
N919	NGC 7479	346.236	12.323	1.65 ± 0.19	SEYFERT	z=0.008;
N920	NGC 7582	349.597	-42.370	5.48 ± 0.59	SEYFERT	z=0.005;
N921	IGR J23206+6431	350.163	64.535	0.80 ± 0.06	SEYFERT	R 333; z=0.072;
N922	Cas A	350.859	58.800	4.31 ± 0.06	SNR	
N923	RX J2325.9+2153	351.503	21.922	1.78 ± 0.25	SEYFERT	z=0.120;
N924	PKS 2325+093	351.933	9.597	1.38 ± 0.30	BLAZAR	z=1.840;
N925	**IGR J23300+8406**	352.500	84.100	2.90 ± 0.59	UNIDENT	!B16;

Table A1 – continued from previous page

Id	Name[1]	RA[2] (deg)	Dec[2] (deg)	Flux[3] (17–60 keV)	Type[4]	Notes
N926	IGR J23308+7120	352.632	71.415	0.64 ± 0.09	SEYFERT	R 1,345,346; z=0.037;
N927	**IGR J23439-2148**	355.990	-21.800	3.11 ± 0.57	UNIDENT	!B16;
N928	1ES 2344+514	356.760	51.700	0.47 ± 0.10	BLAZAR	z=0.044; !B16;
N929	IGR J23523+5844	358.065	58.763	0.64 ± 0.06	SEYFERT	R 333,25,1,58,346; z=0.164;

APPENDIX B: REFERENCES IN THE CATALOG

(1) Masetti et al. (2008), (2) den Hartog et al. (2006), (3) Tomsick et al. (2008), (4) Kuiper et al. (2006b), (5) Eckert et al. (2004), (6) Markwardt et al. (2004), (7) Masetti et al. (2009), (8) den Hartog et al. (2004b), (9) Coe et al. (2015), (10) Rojas et al. (2017), (11) Karasev et al. (2018), (12) Townsend et al. (2011), (13) Burenin et al. (2006b), (14) Bird et al. (2010), (15) Masetti et al. (2010b), (16) Tomsick et al. (2012), (17) Segreto et al. (2013), (18) Halpern & Tyagi (2005), (19) Wang (2010), (20) Rodriguez et al. (2010), (21) Kuiper et al. (2005), (22) Baumgartner et al. (2013), (23) Watson et al. (2009), (24) Burenin et al. (2008), (25) Rodriguez et al. (2008), (26) Bikmaev et al. (2017), (27) Beri et al. (2021), (28) Doroshenko et al. (2020a), (29) Apparao et al. (1978), (30) Baumgartner et al. (2010), (31) Parisi et al. (2012), (32) Bikmaev et al. (2008b), (33) Parisi et al. (2014), (34) Lutovinov et al. (2010b), (35) Lutovinov et al. (2012), (36) Burenin et al. (2006a), (37) Mereminskiy et al. (2016), (38) Oh et al. (2018), (39) Tomsick et al. (2015), (40) Spiro et al. (2013), (41) Krivonos et al. (2011), (42) Martí et al. (2004), (43) Grebenev et al. (2013), (44) Bernardini et al. (2015), (45) Sazonov et al. (2005), (46) Masetti et al. (2006c), (47) Malizia et al. (2016), (48) Vasilopoulos et al. (2014), (49) Vasilopoulos et al. (2013), (50) Revnivtsev et al. (2007), (51) Winter et al. (2008), (52) Bird et al. (2016), (53) Krivonos et al. (2017), (54) Bird et al. (2006), (55) den Hartog et al. (2004a), (56) Landi et al. (2017), (57) Malizia et al. (2012), (58) Sazonov et al. (2008), (59) Revnivtsev et al. (2009), (60) Bernardini et al. (2012), (61) Zurita Heras et al. (2009), (62) Sanna et al. (2017), (63) Landi et al. (2010b), (64) Parisi et al. (2008), (65) Huchra et al. (2012), (66) Tueller et al. (2008), (67) Masetti et al. (2013), (68) Kuiper et al. (2006a), (69) Coleiro et al. (2013), (70) Revnivtsev et al. (2006), (71) Masetti et al. (2006d), (72) Morelli et al. (2006), (73) Masetti et al. (2006a), (74) Leyder et al. (2008), (75) Fiocchi et al. (2010), (76) Fortin et al. (2018), (77) Clavel et al. (2019), (78) Karasev et al. (2020), (79) Bird et al. (2007), (80) Lubiński et al. (2005), (81) Negueruela et al. (2005), (82) Sidoli et al. (2006), (83) Produit et al. (2004), (84) Grebenev et al. (2004), (85) Negueruela et al. (2007), (86) González-Martín et al. (2011), (87) Mescheryakov et al. (2009), (88) Masetti et al. (2010a), (89) Karasev et al. (2012), (90) Krivonos et al. (2018), (91) Oh et al. (2015), (92) Malizia et al. (2017), (93) Tomsick et al. (2021), (94) Chernyakova et al. (2005), (95) Aharonian et al. (2005), (96) Sazonov et al. (2007), (97) Landi et al. (2010a), (98) Krivonos et al. (2007b), (99) Kniazev et al. (2010), (100) Tomsick et al. (2009), (101) D'Aì et al. (2011), (102) Koss et al. (2011), (103) Cornelisse et al. (2002), (104) Keek et al. (2006), (105) Renaud et al. (2010), (106) Landi et al. (2011a), (107) Tomsick et al. (2016a), (108) Bernardini et al. (2018), (109) Molina et al. (2015), (110) Masetti et al. (2006e), (111) Tomsick et al. (2020), (112) Tuerler et al. (2012), (113) Tueller et al. (2010), (114) Tomsick et al. (2016b), (115) Malizia et al. (2010), (116) Milisavljevic et al. (2011), (117) Krimm et al. (2011), (118) Masetti et al. (2007c), (119) Edelson & Malkan (2012), (120) Landi et al. (2011b), (121) Margutti et al. (2019), (122) Walter et al. (2004), (123) Barlow et al. (2006), (124) Masetti et al. (2007b), (125) Tomsick et al. (2006), (126) Soldi et al. (2005), (127) Beckmann et al. (2005), (128) Kuiper et al. (2008), (129) Ratti et al. (2010), (130) Miyasaka et al. (2018), (131) Revnivtsev et al. (2003a), (132) Courvoisier et al. (2003), (133) Tomsick et al. (2003), (134) Lutovinov et al. (2005a), (135) Walter et al. (2006), (136) Negueruela & Schurch (2007), (137) Acero et al. (2015), (138) Revnivtsev et al. (2003c), (139) Nespoli et al. (2010), (140) Bodaghee et al. (2006), (141) Tomsick et al. (2004), (142) Lutovinov et al. (2004b), (143) Lutovinov et al. (2005b), (144) Molkov et al. (2003), (145) Chaty et al. (2008), (146) Grebenev et al. (2005b), (147) Nespoli et al. (2008b), (148) Pearlman et al. (2019), (149) Koss et al. (2017), (150) Hiemstra et al. (2011), (151) Lutovinov et al. (2010a), (152) Burenin et al. (2007), (153) Xiao et al. (2019), (154) Grebenev et al. (2018), (155) Kalamkar et al. (2011), (156) Krivonos et al. (2009), (157) Sanchez-Fernandez et al. (2015), (158) Churazov et al. (2007), (159) Degenaar et al. (2012), (160) Kuulkers et al. (2003), (161) Lutovinov & Revnivtsev (2003), (162) Capitanio et al. (2006), (163) Grebenev et al. (2005a), (164) Grebenev et al. (2007a), (165) Kuznetsova et al. (2019), (166) Landi et al. (2012), (167) Rahoui et al. (2017), (168) Krivonos et al. (2012), (169) Masetti et al. (2012a), (170) Bassani et al. (2005), (171) Caccianiga et al. (2008), (172) Brandt et al. (2006a), (173) Barlow et al. (2005), (174) Sidoli et al. (2011), (175) Barthelmy et al. (2019), (176) Gänsicke et al. (2005), (177) Bozzo et al. (2018a), (178) Lutovinov et al. (2004a), (179) Bozzo et al. (2015), (180) Degenaar et al. (2010), (181) Kuulkers et al. (2006), (182) Goossens et al. (2019), (183) Gibaud et al. (2011), (184) Nucita et al. (2012), (185) Del Santo et al. (2014), (186) Sunyaev et al. (2003a), (187) Smith & Hartigan (2006), (188) Sguera et al. (2020), (189) Britt et al. (2013), (190) Kretschmar et al. (2004), (191) Heinke et al. (2009), (192) Bassani et al. (2004), (193) Torres et al. (2004), (194) Falanga et al. (2011), (195) Krivonos et al. (2013), (196) Bahramian

[1] Name of the source. The sources newly discovered in the hard X-ray domain are highlighted in bold text.

[2] Equatorial coordinates (right ascension and declination) are in the standard J2000.0 epoch.

[3] The measured 17–60 keV flux of the source $\times 10^{-11}$erg cm^{-2}s^{-1}. The flux is highlighted in red colour if the source is detected at $S/N < 4.5\sigma$.

[4] General astrophysical type of the object. A question mark indicates that the specified type should be confirmed.

[5] This column contains notes on the identification and classification of some sources and letter-coded information flags as follows: "R" – comma-separated list of references, which can be found in Sect. B; "z" – redshift; "T" – transient source; "E" – spatially extended source; "C" – spatial confusion with other source, measured flux should be taken with caution; "H" – the source is located in a region with high systematic noise, and its measured flux should be taken with caution; "!B16" – the source has not been found in the *INTEGRAL*/IBIS survey by Bird et al. (2016).

et al. (2014), (197) Heinke et al. (2019), (198) Cocchi et al. (1999), (199) Vovk et al. (2012), (200) Bélanger et al. (2006), (201) Krivonos et al. (2007a), (202) Mori et al. (2015), (203) Mescheryakov et al. (2006), (204) Pavlinsky et al. (1994), (205) Revnivtsev et al. (2003b), (206) Kalemci et al. (2006), (207) in 't Zand et al. (1998), (208) Zolotukhin & Revnivtsev (2015), (209) Brandt et al. (2006b), (210) Wijnands (2006), (211) Degenaar et al. (2007), (212) Kaur et al. (2017), (213) Grebenev et al. (2005c), (214) Del Monte et al. (2008b), (215) Altamirano et al. (2008), (216) Del Monte et al. (2008a), (217) Zhang et al. (2009), (218) Revnivtsev et al. (2004b), (219) Terrier et al. (2010), (220) Zhang et al. (2015), (221) Rodriguez et al. (2009), (222) Malizia et al. (2007), (223) Grebenev & Sunyaev (2007), (224) Zurita Heras & Chaty (2008), (225) Karasev et al. (2010), (226) Kaur et al. (2010), (227) Nebot Gómez-Morán et al. (2015), (228) Scott et al. (1997), (229) Brandt et al. (2008), (230) Soldi et al. (2006), (231) Paizis et al. (2007), (232) Rodriguez et al. (2007), (233) Papitto et al. (2011), (234) Ferrigno et al. (2011), (235) Bozzo et al. (2011), (236) Greiss et al. (2011), (237) Russell et al. (2011), (238) Chakrabarty et al. (2011b), (239) Zolotukhin & Revnivtsev (2011), (240) Revnivtsev et al. (2008), (241) Grebenev & Sunyaev (2004), (242) Natalucci et al. (2011), (243) Grebenev et al. (2019), (244) Hare et al. (2021), (245) Morgan et al. (2005), (246) Neustroev et al. (2014), (247) Shaw et al. (2017), (248) Kuulkers et al. (2013), (249) Krimm et al. (2013b), (250) Krimm et al. (2013a), (251) Chelovekov & Grebenev (2007), (252) Sunyaev et al. (2003b), (253) in't Zand (2005), (254) Curran et al. (2011), (255) Ducci et al. (2018), (256) Sanna et al. (2018), (257) Lutovinov et al. (2003b), (258) Brandt et al. (2007), (259) Coughenour et al., (in prep.), (260) Revnivtsev et al. (2004a), (261) Torrejón et al. (2010), (262) Masetti et al. (2004), (263) Chenevez et al. (2012), (264) Nucita et al. (2007), (265) Masetti et al. (2012b), (266) Del Santo et al. (2011), (267) Chakrabarty et al. (2011a), (268) Kaur et al. (2011), (269) Negoro et al. (2018), (270) Fuerst et al. (2018), (271) Rau (2018), (272) Armas Padilla et al. (2019), (273) Ubertini et al. (2005), (274) Funk et al. (2007), (275) Burenin et al. (2009), (276) Worpel et al. (2020), (277) Nabizadeh et al. (2019), (278) Halpern & Gotthelf (2008), (279) Bozzo et al. (2018b), (280) Butler et al. (2009), (281) Fornasini et al. (2017), (282) Cusumano et al. (2020), (283) La Parola et al. (2013), (284) Markwardt (2008), (285) Eckert et al. (2013), (286) Bassani et al. (2006), (287) Landi et al. (2009), (288) Nakahira et al. (2013), (289) Oda et al. (2019), (290) Clavel et al. (2016), (291) Bassani et al. (2009), (292) Lutovinov et al. (2003a), (293) Ferrigno et al. (2012), (294) Malizia et al. (2005), (295) Pavlinsky et al. (2021), (296) Rodriguez et al. (2004), (297) Nespoli et al. (2008a), (298) Doroshenko et al. (2020b), (299) Krimm et al. (2012), (300) McCollum & Laine (2019), (301) Kennea et al. (2019), (302) Grebenev et al. (2007b), (303) Grebenev & Sunyaev (2010), (304) Bodaghee et al. (2012), (305) Sguera et al. (2013), (306) Kuiper & Hermsen (2009), (307) Chernyakova et al. (2003), (308) Molkov et al. (2004), (309) Terrier et al. (2008), (310) Reynolds et al. (2012), (311) Bikmaev et al. (2006), (312) Kaaret et al. (2006), (313) Karasev et al. (2007), (314) Karasev et al. (2008), (315) Xu et al. (2019), (316) Stephen et al. (2018), (317) Halpern & Thorstensen (2018), (318) Halpern et al. (2018), (319) Hannikainen et al. (2003), (320) Pavan et al. (2011), (321) Krivonos et al. (2010b), (322) Tueller et al. (2005), (323) Degenaar et al. (2011), (324) Steeghs et al. (2008), (325) Rodes-Roca et al. (2018), (326) Torres et al. (2006), (327) Hare et al. (2019), (328) Tovmassian et al. (2017), (329) Masetti et al. (2007a), (330) Halpern (2006), (331) Bassani et al. (2014), (332) Goncalves et al. (2008), (333) Bikmaev et al. (2008a), (334) Masetti et al. (2006b), (335) Winter et al. (2009), (336) Westergaard et al. (2006), (337) Landi et al. (2011c), (338) Maselli et al. (2013), (339) Gianní et al. (2011), (340) Lamperti et al. (2017), (341) Bassani et al. (2007), (342) Masetti et al. (2012c), (343) Esposito et al. (2013), (344) Lutovinov et al. (2013), (345) Landi et al. (2007), (346) de Rosa et al. (2012).

This paper has been typeset from a TEX/LATEX file prepared by the author.